Omega 138 (2026) 103428

Contents lists available at ScienceDirect

Omega

journal homepage: www.elsevier.com/locate/omega

Optimizing election logistics: A multi-period routing problem embedding time-dependent reward functions☆

Renata Mansini [a], Lorenzo Moreschini [a,*,1], Mesut Sayin [b]

[a] Department of Information Engineering, University of Brescia, Via Branze 38, 25123, Brescia, Italy
[b] Faculy of Business, Özyeğin University, Nişantepe, Çekmeköy, 34794, İstanbul, Turkiye

ARTICLE INFO

Dataset link: https://github.com/lmores/or-rmprp-data

Keywords:
Multi-period politician routing problem
US elections
Time-dependent rewards
Generalized subtour elimination constraints
Mixed-integer linear programming

ABSTRACT

With the 2024 US Presidential Election now concluded, the growing complexity of designing effective election campaigns has become clearer. Motivated by the logistical challenges associated with US election campaigns, we introduce the Reward-driven Multi-period Politician Routing Problem. It involves diverse politicians planning their campaigns over multiple days, considering constraints such as clustered locations, time- and location-dependent rewards, budget limits, mandatory rest days, and flexible daily routes that can be either open or closed, with starting and ending locations not known in advance.

We model the problem as a mixed-integer linear program, complemented with several valid inequalities, and innovate by designing new subtour elimination techniques that jointly deal with open and closed paths. We developed 36 new benchmark instances tailored to the US presidential elections. To tackle large-sized instances, we develop a Sequential Route Construction Matheuristic that exploits the multi-period structure of the problem to provide efficient and effective solutions. We incorporate time-dependent reward profiles (concave, convex, linearly decreasing, linearly increasing, and periodic) into the objective function to capture diverse decision-making perspectives. Experimental results show interesting computational issues on the different tested models and the impact of the chosen reward profile on their performance.

1. Introduction

Planning an election campaign for several politicians of the same party requires balancing a complex range of constraints and objectives, leading to significant logistical challenges and high costs. Nowadays, in the US, both major political parties spend billions on advertising, logistics, and traveling expenses for candidates [1] to achieve successful political campaigns. The cost of running for president has increased by more than 1000% since 1976.[2] During the 2020 US presidential election, candidates and their respective political parties collectively spent over \$14 billion.[3] Moreover, in 2020, the average Senate campaign spent \$15.8 million, and the average House campaign totaled \$2.3 million.[4] Such financial stakes escalated further in the 2024 US elections, where campaign spending reached unprecedented levels, with estimates suggesting total expenditures well over \$16 billion across federal elections, setting a new record[5,6]. These high costs emphasize the need to address the challenge of optimizing the routing and scheduling of election campaigns, especially considering real-world constraints, a relatively unexplored area in the existing literature.

Current models in the routing literature often fail to capture the full complexity of election logistics. Multi-period variants of the Team Orienteering Problem [2,3] and heterogeneous vehicle routing problems [4,5] typically rely on restrictive assumptions, such as fixed depots, static rewards, and mandatory tour completion at specific nodes. These assumptions do not fit well with election logistics. In this paper, motivated by real-life challenges in managing election campaigns, we introduce the Reward-driven Multi-period Politician Routing

☆ Area: Transportation and Logistics. This manuscript was processed by Associate Editor Teobaldo Bulhões.
* Corresponding author.
E-mail addresses: renata.mansini@unibs.it (R. Mansini), lorenzo.moreschini@unibs.it (L. Moreschini), mesut.sayin@ozyegin.edu.tr (M. Sayin).
1 The review phase of this article took place while this author was affiliated with the Polytechnic University of Milan, Department of Design, Via Giovanni Durando 10, 20158, Milan, Italy.
2 https://www.brennancenter.org/our-work/analysis-opinion/most-expensive-election-ever
3 www.bbc.com/news/av/election-us-2020-54696386
4 www.reuters.com/graphics/USA-ELECTION/SENATE-FUNDRAISING/yxmvjeyjkpr/
5 www.opensecrets.org/news/2024/10/total-2024-election-spending-projected-to-exceed-previous-record
6 www.usnews.com/news/national-news/articles/2024-11-01/16-billion-will-be-spent-in-the-2024-election-wheres-it-all-going

https://doi.org/10.1016/j.omega.2025.103428
Received 6 April 2025; Accepted 12 September 2025
Available online 19 September 2025

Problem (RM-PRP) to tackle the problem of designing an optimal election campaign itinerary for multiple candidates of the same party throughout an election campaign under various resource constraints. We apply the RM-PRP and the proposed solution methods to the US presidential elections, although they are also adaptable to general and primary elections in other countries.

In RM-PRP, the locations to visit are partitioned into clusters, reflecting the tendency in the 2024 US presidential election to group states or regions for campaign activities. This approach ensures a balanced geographical cover, signaling inclusion and concern for all constituencies, even in areas where a party's prospects may appear limited. For example, Democratic candidates invested significant time in traditionally Republican states to showcase a commitment to reaching all US citizens, regardless of the likely outcomes. This highlights the role of both practical and symbolic activities in a campaign strategy. In addition, recent campaigns indicate that decision-making in election logistics often diverges from straightforward optimization models: political parties appear to adopt more complex and nuanced mental optimization frameworks, mainly based on reward functions of various types. To capture this diversity while preserving linear models, RM-PRP considers different objective functions that embed time-dependent reward profiles and clustering of locations.

The RM-PRP aims to plan election campaigns that span multiple days. Locations are grouped into clusters and traveling between locations incurs specific costs and travel times. Each location is associated with an activity cost and duration, an overnight stay cost, and a base reward depending on the politician who holds an activity in that location. The realized rewards are influenced by a time-dependent function and penalties apply to the rewards for subsequent activities in the same location, contingent on the number of days elapsed since the previous one, promoting careful planning. Politicians operate within budget constraints and must return to their campaign center regularly, incorporating rest days into their schedules. They are also limited to a predefined number of meetings per day and must meet minimum engagement requirements within each cluster. The goal of RM-PRP is to maximize the total cumulative rewards collected by all politicians through the first activities and subsequent ones. In this paper, the term *activity* refers to various voter engagement events, such as town hall meetings, rallies, public events, one-on-one meet-and-greet sessions, debates to present policies and interact with other candidates, and interviews to reach a broader audience. In our model, these activities are treated uniformly by assigning the same reward to a city regardless of the type of engagement.

The practical significance of the RM-PRP is evident from historical campaign missteps. For instance, during the 2016 US presidential election, Hillary Clinton's campaign failed to allocate sufficient time to critical swing states like Wisconsin and Michigan in the final days, despite their pivotal electoral weight. Clinton did not visit Wisconsin once after the Democratic National Convention, while her opponent held multiple rallies there. This logistical oversight is widely cited as a contributing factor to her narrow losses in these states and, ultimately, the election [6]. The RM-PRP could have mitigated such risks by optimizing travel routings and schedules to prioritize high-reward states under resource constraints to ensure no critical area was overlooked.

As a case study, we consider the US presidential election, where multiple politicians campaign in US states to deliver speeches and hold political meetings. In the US, the typical duration of the final phase of presidential election campaigns is usually less than a few months [7]. This number drops below 40 days in most European countries [8]. As a result, the campaign team must carefully manage their time and resources to reach as many voters as possible within the allotted time. Another constraint is budget: campaigns can be expensive, and each candidate has a limited budget to work with, taking into account the cost of travel, accommodation, venue rents, and other expenses. Accordingly, RM-PRP imposes a budget limit on the total spending of each politician. We consider separate budget limits for each candidate as candidates operate with distinct fundraising capacities, spending limits, and strategic roles within a party. Top nominees require larger budgets because they lead high-impact activities like major rallies and media campaigns, which demand significant resources for travel, security, and outreach. Additionally, political parties often have more than one politician running for office in order to increase their chances of winning. Having multiple candidates on the ballot can help to broaden the party's appeal to different demographics and regions. For general elections, the presence of multiple politicians in RM-PRP can be equated to presidential and vice-presidential candidates, campaign managers, and other key figures. RM-PRP accommodates these limitations by integrating relevant constraints into the model.

Although developed for election campaigns, RM-PRP's features make it applicable to other domains requiring coordinated routing and scheduling across multiple travelers and time periods. For instance, in planning tourist trips, travel agencies that organize itineraries for groups of tourists across clustered attractions can use RM-PRP to optimize routes and schedules. In this application, attractions are clustered by theme or location, rewards are time-dependent (e.g., sunset views at beaches or nighttime monument tours), and routes may be open/closed as travelers change hotels. Constraints like distinct budgets for different groups of travelers, mandatory rest periods between intensive days, and optional repeat visits to key sites (e.g., revisiting the Eiffel Tower at different times) mirror the RM-PRP's key features. Similarly, mobile healthcare services (e.g., vaccination buses or rural medical units) must visit dispersed communities under budget constraints, while adhering to rest cycles and time-dependent demands. Another relevant setting is humanitarian logistics, such as post-disaster response teams delivering aid in different phases. Clustered nodes (e.g., regions or neighborhoods), urgency-driven time-dependent rewards (e.g., 72 hours golden time to rescue people trapped under debris, during which survival rates decline sharply), and travel/rest limits in RM-PRP are well-suited to capture the operational realities of such missions.

The RM-PRP is an extension of the recently introduced Roaming Salesman Problem (RSP) [9]. The presence of multiple politicians introduces additional complexity compared to the RSP in which a single one is involved. This complexity is emphasized in [10] where the authors address a variant of the problem (mRSP) involving more than one politician. RM-PRP differs from mRSP in the following ways:

1. RM-PRP extends the RSP by accommodating the presence of multiple politicians, each of whom is assigned distinct budget allocations for the election campaign. In [10], the presence of multiple travelers is also considered, but a single shared budget is assumed, and no distinctions are made between politicians, who are therefore modeled as homogeneous vehicles. The RM-PRP acknowledges the differences among party delegates, recognizing that a speech given by the presidential candidate carries more weight than those given by the running mate or press secretary. Consequently, the rewards collected by politicians are aligned with the significance of their roles. Typically, this hierarchy of importance in general elections places the main candidate at the top, followed by the vice presidential candidate/running mate, and then the press secretary, in descending order of importance.
2. Differently from previous literature, in the RM-PRP, cities are grouped into clusters based on their resistance to switching party support. This means that areas with a strong historical commitment to a particular political party are less likely to change their support to the opposing party, even when new political dynamics arise. The clustering reflects the fact that certain cities exhibit a higher degree of loyalty to a political party, making them less vulnerable to shifts in political trends. By grouping cities in this way, we can better represent how party loyalty varies between different areas and how resistant these areas are to political transformations. In RM-PRP, politicians comply with

the requirement to hold activities in at least a specified number of cities within each cluster, accounting for social and political factors, ensuring a more balanced geographical distribution.

3. The RSP solely focuses on time-dependent rewards that decrease as the election date draws near. Similarly, mRSP accounts for a unique time-dependent trend of the reward corresponding to a linearly increasing function. However, political experts hold varying opinions on this matter: while some experts argue that the significance of meetings escalates over time, others contend that it diminishes. Furthermore, some others propose that the importance of meetings initially declines and then rises again as time progresses. To capture all these diverse viewpoints, we generalize previous problems by introducing five distinct time-dependent reward functions: non-linear concave, non-linear convex, linearly decreasing, linearly increasing, and periodic.
4. In mRSP, activities can be held more than once and, in each city, the problem counts the first activity of each politician separately, treating each one as equally rewarding. Subsequent activities incur penalties based on the time elapsed since the previous one, with specific constraints that prevent holding another activity within a certain number of days, depending on who made the prior activity. RM-PRP introduces a key innovation by defining a single "first activity" for each city, regardless of which politician performs it. All subsequent activities are penalized based on the time elapsed since the previous one, regardless of who performs them. This approach allows for a more precise evaluation compared to the previous model, as it captures the strategic significance of the initial engagement while reflecting the diminishing value of repeated activities over time, more accurately representing the real-world campaign strategies employed by a political party.
5. In contrast to mRSP, the RM-PRP introduces restrictions not only on expenses related to accommodation but also on travel costs and holding political events. We define a total budget for each politician for the entire duration of the election campaign to ensure that all campaign-related costs remain within their limits.
6. In mRSP, there is a rigid requirement to conduct at least one meeting per day. Nevertheless, reviewing the actual schedules of politicians during the 2020 and 2024 US presidential elections, we observe the inclusion of intermittent rest days between meetings. Recognizing this pattern, RM-PRP introduces a more flexible approach by relaxing this constraint. Politicians are now permitted to incorporate rest days between their schedules of meetings.
7. While the objective function of mRSP includes travel costs by maximizing the difference between collected rewards and traveling expenses, it is evident that this aspect is not the foremost concern for political parties. Our observations indicate that a significant portion of their travel is facilitated through private jets or chartered flights, which implies that travel cost is a second-order issue. Hence, in RM-PRP, we have redefined the objective function that only maximizes the collected reward, binding travel expenses in the constraints.

The contributions of this paper can be summarized as follows. First, motivated by the complexity of US presidential election campaigns, we introduce a new optimization problem that coordinates the routing and scheduling of multiple politicians from the same party. In this problem, cities are grouped into clusters, and the objective is to maximize the total (time-dependent) rewards, with the highest values placed on the first activity in each city. This problem is of both practical and theoretical significance, presenting substantial computational challenges and the potential to improve the effectiveness of election logistics. Second, by incorporating different time-dependent reward functions, the model captures diverse decision-making perspectives, allowing for the representation of varying strategic priorities set by campaign planners. This approach extends classical routing problems by integrating unique features tailored to real-world political campaign dynamics. Third, we develop both compact and non-compact formulations of the problem. In particular, the compact MILP formulation builds on the existing mRSP, incorporating the new condition on the first activities and additional real constraints. Similarly to the mRSP, this formulation simultaneously handles open, closed, and no tours on the same day for different politicians, using the Miller-Tucker-Zemlin (MTZ) constraints for subtours elimination. In this work, we refine the formulation, dropping the need to introduce a fictitious node and simplifying many related constraints. We also develop generalizations of Connectivity Constraints (CC) and Subtour Elimination Constraints (SEC). These new formulations deal with the presence of meshed tour-type choices further complicated by time-dependent rewards and temporal constraints on activities in the same city. All formulations have been tested and compared, providing interesting conclusions on their performance. Fourth, we develop and test different families of valid inequalities. Fifth, we conduct an extensive computational analysis and compare the different reward functions and their impact on the solutions.

The remainder of this paper is organized as follows. In Section 2, we review the relevant literature. In Section 3, we provide the problem description, whereas in Section 4 we present the mathematical programming formulations. We discuss the methods used to eliminate subtours in Section 5, followed by an explanation of valid inequalities in Section 6. The developed matheuristic algorithm is presented in Section 7, with computational experiments detailed in Section 8. We conclude the paper in Section 9.

2. Literature review

The Reward-driven Multi-period Politician Routing Problem (RM-PRP) is a challenging NP-hard optimization problem, which extends the Roaming Salesman Problem (RSP) by considering multiple vehicles. The RM-PRP is also a generalization of the Team Orienteering Problem (TOP) [11], a selective routing problem that incorporates profits associated with the locations to visit. TOP and its variants have found numerous applications in vehicle routing and tourist trip planning [12–16]. However, there is a relatively limited exploration of the TOP in other domains, such as political campaign logistics and marketing [10,17–19]. Both the Traveling Salesman Problem (TSP) and its variants, including the RSP, mRSP, and TOP, are known to be NP-hard problems, making it computationally demanding to find optimal solutions [20].

The RM-PRP can be considered as part of the family of rich routing problems, i.e., problems including real-life features not considered in the basic Capacitated Vehicle Routing Problem. In particular, it incorporates a planning horizon made of multiple periods (days), variable daily depots, and parameters depending on time. Time dependency introduces new challenges in routing problems, as travel times, collected rewards, or other factors may vary based on temporal and contextual elements. For instance, [21] explore a time-dependent vehicle routing problem in a road network where travel times are influenced by departure times and traffic congestion, focusing on the impact of temporal variations on cost efficiency and fuel consumption. Similarly, [22] addresses the multi-trip time-dependent vehicle routing problem with time windows that incorporates factors such as multiple trips per vehicle, time windows, and loading times at depots. The study highlights the complexity introduced by time-dependent travel functions, which require tailored techniques to minimize travel distances while adhering to constraints like capacity and trip durations. Focusing on time dependency, other studies examine how temporal variations in rewards or service conditions influence routing decisions. The authors in [23] investigate the time-varying reward Orienteering Problem where vertex rewards fluctuate over time, which necessitates optimal timing to maximize collected rewards within path length constraints.

Similarly, [24] focuses on the time-dependent Orienteering Problem with time windows and service time-dependent profits, illustrating how extended service times can enhance profits, depending on available time budgets and travel time constraints. In their model, each node is associated with lower and upper service time bounds, and the reward increases linearly with the time spent at the node, allowing higher profits for longer visits. In contrast, our study considers five distinct time-dependent reward profiles, including linear and nonlinear shapes. We also introduce penalties for repeated visits to the same node, based on the number of days elapsed since the previous visit. Unlike [24], which assumes a minimum visit duration to secure a baseline reward (with longer visits yielding a greater profit), our reward collection is independent of service time.

Several other studies in the literature further illustrate the diverse applications of time-dependent routing problems by emphasizing their practical significance across various domains. For instance, [25] introduce a secure time-dependent vehicle routing problem, which considers uncertain demands and integrates security risks with time-dependent travel speeds. In [26], the authors focus on real-time adjustments in time-dependent delivery plans by emphasizing the importance of minimizing disruptions while responding dynamically to changes in travel times. Similarly, [27] propose a truck-drone hybrid routing problem with time-dependent travel times to show the potential of integrating drones to enhance delivery efficiency under uncertain traffic conditions. Finally, [28] address the time-dependent green vehicle routing problem for cold-chain logistics by incorporating temporal and spatial traffic dynamics to minimize costs related to transportation, refrigeration, and carbon emissions.

RM-PRP distinguishes itself from closely related problems by simultaneously integrating multiple features that are typically addressed separately in the routing literature. Unlike the standard TOP or its multi-period extensions [2], which often assume homogeneous agents [29], RM-PRP models heterogeneous agents with individualized budgets, roles, and constraints. Compared to the mRSP [10], RM-PRP introduces inter-agent differentiation, cluster-level coverage constraints, and flexible temporal engagement rules that more accurately reflect how speech tours are planned in practice. While capacitated VRP handles vehicle load and service limits [30], it rarely incorporates penalties for repeated visits featured in RM-PRP. Moreover, classical orienteering and vehicle routing models typically impose fixed depot returns and daily tour completion, which are relaxed in the RM-PRP to allow both open and closed paths, or no travel at all.

3. Problem definition

In this section, we define the Reward-driven Multi-period Politician Routing Problem (RM-PRP), which aims to optimally plan the activities of various politicians for a multi-period campaign across different cities under several constraints.

Let $T = \{1, \dots, \bar{t}\}$ be the set of days, where $\bar{t} \in \mathbb{N}^+$ represents the total number of days in the campaign planning horizon. We denote as $M = \{1, \dots, \overline{m}\}$ the set of heterogeneous politicians (main election candidates, running mates, and party representatives). The RM-PRP is defined on a directed graph $G = (N, A)$ with node set $N = \{1, \dots, \overline{n}\}$ and arc set $A \subseteq \{(i, j) \mid i, j \in N,\ i \neq j\}$. Each node represents a city[7] that can be visited, with node 1 serving as the campaign center. The set N is partitioned into a family of $\overline{k} \in \mathbb{N}^+$ non-empty subsets N_1, N_2, …, $N_{\overline{k}}$, indexed by the set $K = \{1, \dots, \overline{k}\}$, such that $\bigcup_{k\in K} N_k = N$ and $N_k \cap N_l = \emptyset$ for each $k, l \in K$ with $k \neq l$. Each subset N_k represents the set of cities belonging to cluster $k \in K$. In our application, the clustering criterion is based on the similarity in cities' resistance to switching political parties, as inferred from their historical voting patterns. Each arc $(i, j) \in A$ is associated with a travel cost $c_{ij} \in \mathbb{R}^+$ and a travel time $d_{ij} \in \mathbb{R}^+$. Each city $i \in N$ is associated with an activity duration $a_i \in \mathbb{R}^+$, indicating the time required to hold a political meeting in i. Each politician $m \in M$ starts from an initial city $s_m \in N$ on day $t = 1$ and can visit any city, but no two politicians can hold activities in the same city on the same day. On different days, a city can host multiple activities, each assigned to any politician. Overnight stays in a city are allowed without activities, so visits do not always yield rewards.

A time-dependent reward is collected in city $i \in N$ if a politician performs an activity in that city on a given day. The realized value of the reward depends on the politician $m \in M$, the city $i \in N$, the day $t \in T$, and also on the time passed since the last activity held in the same city (by any politician). For this reason, we introduce two families of rewards: the rewards $r_{mit} \in \mathbb{R}^+$ collected when the very first activity is held by any politician m in city i on day t, and the rewards $r'_{mits} \in \mathbb{R}^+$ collected when a subsequent activity is held by politician m in the same city i on day t and $s \in \mathbb{N}^+$ $(s \leq t-1)$ days after the previous one (held by any politician).

To model both types of rewards in a unified way, we express them in terms of a base reward $\tilde{r}_{mi} \in \mathbb{R}^+$ associated with politician $m \in M$ and city $i \in N$. Specifically, we assume:

$$r_{mit} = \tilde{r}_{mi} \cdot \Phi(t),$$

where $\Phi(t)$ is a generic time-dependent modulation function defined over the campaign horizon $t \in T$. Similarly, in the case of repeated visits to the same location, we define:

$$r'_{mits} = \tilde{r}_{mi} \cdot \Phi'(t, s),$$

where $\Phi'(t, s)$ accounts for the change of the reward given by holding an activity on day $t \in T$, when the previous one (by any politician) took place $s \in \mathbb{N}^+$ days before. The functions Φ and Φ' are intentionally left undefined in the problem formulation and may be selected by the decision maker to reflect diverse strategic priorities or political beliefs about the evolution of campaign impact over time. For instance, some campaign planners may consider early visits to be most effective, others may value visibility closer to the election date, while yet others may assume non-monotonic or periodic patterns of voter engagement. This modeling flexibility allows RM-PRP to embed various temporal reward dynamics in a unified optimization framework. The specific reward profiles used in our computational experiments (covering five distinct patterns: concave, convex, increasing, decreasing, and periodic) are introduced in Section 8.1.

The RM-PRP aims to design an optimal $\bar{t}$-day campaign plan for $\overline{m}$ politicians such that the total collected reward is maximized while complying with the following constraints: (i) No politician can exceed the maximum number $p \in \mathbb{N}$ of activities per day (ii) There must be at least $p_{mk} \in \mathbb{N}$ activities among cities in cluster $k \in K$ by politician $m \in M$ (iii) The total duration of each daily tour, including activity time, cannot exceed the maximum tour duration $q \in \mathbb{R}^+$ (iv) If a politician holds an activity in a city $i \in N$ on a day $t \in T$, the same politician cannot hold another activity in the same city in the next $w \in \mathbb{N}$ days; (v) Two activities held in the same city must be separated by at least $l \in \mathbb{N}^+$ days; (vi) The total cost of traveling, holding activities, and overnight stays for each politician $m \in M$ should not exceed the budget $b_m \in \mathbb{R}^+$; (vii) Each politician should have at least $e \in \mathbb{N}$ rest days (not holding activities, although traveling is allowed) every $g \in \mathbb{N}^+$ days $(e \leq g)$ (viii) Each politician must spend a night at the campaign center at least once every $u \in \mathbb{N}^+$ days. Table 1 summarizes the problem notation.

Although the time domain is discrete and finite ($\bar{t}$ days), the interaction between the reward profiles, the multi-agent routing decisions, and the diminishing returns from repeated visits results in a dynamic optimization environment. In this context, the time-dependent reward profiles Φ and Φ' play a central role, as they embody the decision maker's strategic expectations about the future value of political activities. The choice of Φ and Φ' influences whether it is more advantageous

[7] In this article we will use the terms *node* and *city* interchangeably, preferring the former when focusing on the combinatorial structure of the problem and the latter when referring to its real-world application.

Table 1
Notation for the RM-PRP.

Parameter	Description
$M = \{1, \dots, \bar{m}\}$	The set of politicians
$N = \{1, \dots, \bar{n}\}$	The set of cities
$T = \{1, \dots, \bar{t}\}$	The set of days in the planning horizon
$K = \{1, \dots, \bar{k}\}$	The set of cluster indexes
$\{N_k\}_{k\in K}$	The family of (non-empty) clusters, a partition of N
$G = (N, A)$	The directed graph with node set N and arc set $A \subseteq \{(i,j) \mid i, j \in N,\ i \neq j\}$
$a_i \in \mathbb{R}^+$	The duration of an activity in node $i \in N$
$b_m \in \mathbb{R}^+$	The budget of politician $m \in M$ for the entire campaign period
$c_{ij} \in \mathbb{R}^+$	The traveling cost from node $i \in N$ to node $j \in N$ for each $(i,j) \in A$
$d_{ij} \in \mathbb{R}^+$	The traveling time from node $i \in N$ to node $j \in N$ for each $(i,j) \in A$
$e \in \mathbb{N},\ g \in \mathbb{N}^+$	Each politician must rest at least e days every g consecutive days ($e \leq g$)
$h_i \in \mathbb{R}^+$	The cost of holding an activity in node $i \in N$
$l \in \mathbb{N}^+$	The minimum number of days between two activities in the same city by any politician
$o_i \in \mathbb{R}^+$	The cost of the overnight stay in node $i \in N$
$p_{mk} \in \mathbb{N}$	The minimum number of activities in cluster $k \in K$ required for politician $m \in M$
$p \in \mathbb{N}$	The maximum number of activities allowed daily for each politician
$q \in \mathbb{R}^+$	The maximum total duration of the daily tour and activities of a politician
$\tilde{r}_{mi} \in \mathbb{R}^+$	The base reward associated with politician $m \in M$ and city $i \in N$
$r_{mit} \in \mathbb{R}^+$	The reward collected by politician $m \in M$ holding the first activity in city $i \in N$ on day $t \in T$
$r'_{mits} \in \mathbb{R}^+$	The reward collected by politician $m \in M$ when holding an activity in city $i \in N$ on day $t \in T$, s days after the previous one ($l \leq s \leq t-1$)
$s_m \in N$	The initial city of politician $m \in M$ on day $t = 1$
$u \in \mathbb{N}^+$	Each politician must spend at least one night at the campaign center every u consecutive days
$w \in \mathbb{N}^+$	The minimum number of days between two activities in the same city by the same politician

to anticipate or delay a visit to a city, thus shaping the temporal deployment of the campaign and introducing a layer of dynamic complexity into the planning process.

We now present a simple example based on a small RM-PRP instance involving 3 politicians (A, B, and C), 9 cities, 3 clusters, and a 3-day planning horizon. In this instance, we assume unitary costs for travels, activities, and overnight stays and assign each politician a budget of 12 units. Each activity is assumed to last one hour, and the travel time on each arc is set to two hours. Additionally, we impose a maximum of three activities per day ($p = 3$) and a daily route duration limit of nine hours ($q = 9$). Politicians are required to take a rest day ($e = 1$) every three days ($g = 3$), and the minimum number of days between two consecutive activities in the same city must be at least two, regardless of the politician who carries them out ($l = w = 2$). Also, each politician must spend at least one night at the campaign center every three days ($u = 3$). Finally, we impose that each politician must carry out at least two activities in a specific cluster: politician A in the first cluster ($p_{A1} = 2$), politician B in the second cluster ($p_{B2} = 2$), and politician C in the third cluster ($p_{C3} = 2$).

Fig. 1 shows a feasible solution for the above RM-PRP instance. On day 1, politician A leaves the campaign center and travels an open path holding activities in cities i_4 and i_6, spending the night there. Politician B holds a single activity in city i_2 and stays in city i_8 for the first night, while politician C travels directly to city i_9 where they spend the night and do not hold any activity, hence the first day counts as a rest day for politician C. On day 2, politician A leaves i_6 to hold an activity in i_3 and stops at the campaign center for the night; politician B takes a rest day without moving from i_8; and politician C follows a closed path starting from i_9, visiting i_7 and i_5, coming back to i_9 and holding an activity in each city (note that on this day politician C reaches the maximum number of allowed activities and the maximum route duration). On day 3, politician A leaves the campaign center and takes a rest day in i_3; politician B starts taking an activity in city i_8 where they stayed for the night, takes another activity in i_4 (where the previous activity was held 2 days before by politician A) and spends the night at the campaign center; finally, politician C travels to the campaign center where they hold an activity and spend the night.

At the end of the 3-day campaign period, each representative has rested for at least one day, has stayed at the campaign center for at least one night, and they all satisfied the required minimum number of activities in the different clusters.

4. Mathematical formulation

In this section, we provide a mathematical formulation for the RM-PRP. We first describe the objective function and all basic constraints. Then, in Section 5, we deal with alternative formulations of the constraints aimed at avoiding subtours. Finally, in Section 6, we discuss some classes of valid inequalities.

The list of model variables and their meaning is reported in Table 2. Note that S_{mit} ($m \in M$, $i \in N$, $t \in T$) is not defined for $t = 0$. Thus, for each $m \in M$ and $i \in N$, we define S_{mi0} as parameters we use to ensure that each politician starts their path from the respective initial city on day $t = 1$, i.e. for each $m \in M$, we set $S_{ms_m0} = 1$ and $S_{mi0} = 0$ for each $i \in N \setminus \{ s_m \}$.

We now present the core mathematical model for the RM-PRP. Due to the high number of constraints, we introduce them step-by-step in paragraphs that group constraints involving the same families of variables.

$$\max \sum_{m\in M}\sum_{i\in N}\sum_{t\in T} r_{mit}F_{mit} + \sum_{m\in M}\sum_{i\in N}\sum_{t\in T}\sum_{l\leq s\leq t-1} r'_{mits}R_{mits} \tag{1}$$

The objective function consists of two components: the first one accounts for the rewards associated with the first activity in each city, whereas the second refers to the rewards of the subsequent activities.

$$\sum_{i\in N} Z_{mit} \leq p, \qquad \forall m \in M,\ \forall t \in T, \tag{2}$$

$$\sum_{m\in M}\sum_{v=t}^{t+l-1} Z_{miv} \leq 1, \qquad \forall i \in N,\ \forall t \in T : 1 \leq t \leq \bar{t} - l + 1, \tag{3}$$

$$\sum_{v=t}^{t+w-1} Z_{miv} \leq 1, \qquad \forall m \in M,\ \forall i \in N,\ \forall t \in T : 1 \leq t \leq \bar{t} - w + 1, \tag{4}$$

$$\sum_{i\in N_k}\sum_{t\in T} Z_{mit} \geq p_{mk}, \qquad \forall m \in M,\ \forall k \in K. \tag{5}$$

Constraints (2)–(5) involve only the family of variables Z. Constraints (2) ensure that each politician performs at most $p \in \mathbb{N}$ activities on each day. Constraints (3) guarantee a gap of at least $l \in \mathbb{N}^+$ days between subsequent activities held by any politician in the same city $i \in N$ and, in particular, allow at most one activity in each city on any day. Similarly, constraints (4) guarantee that the same politician cannot perform another activity in the same city before w days since their last one. Constraints (5) ensure that by the end of the campaign,

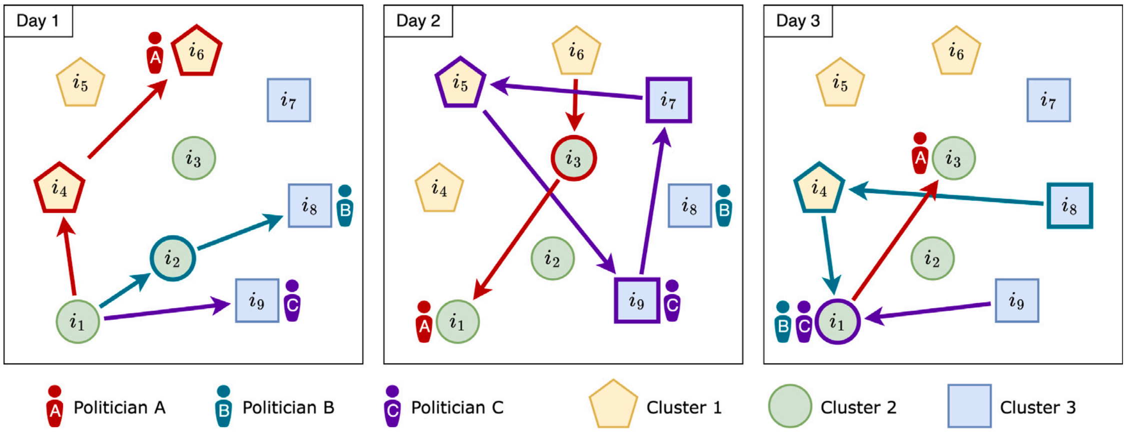

Fig. 1. A feasible solution for a RM-PRP instance with 3 politicians, 9 cities, 3 clusters, and spanning 3 days. Thick node outlines denote activities held in that node by the politician associated with the same color of the outline. Politicians' icons appear close to the city where they stop for the night (possibly holding no activity).

Table 2
Variables of the mathematical model.

Variable	Description
$E_{mit} \in \{0,1\}$	1 if politician $m \in M$ enters but does not leave node $i \in N$ on day $t \in T$, 0 otherwise
$F_{mit} \in \{0,1\}$	1 if the first activity in city $i \in N$ is performed by politician $m \in M$ on day $t \in T$, 0 otherwise
$J_{mt} \in \{0,1\}$	1 if politician $m \in M$ traverses an open path on day $t \in T$, 0 otherwise
$L_{mit} \in \{0,1\}$	1 if politician $m \in M$ leaves but does not enter node $i \in N$ on day $t \in T$, 0 otherwise
$R_{mits} \in \{0,1\}$	1 if politician $m \in M$ holds an activity in city $i \in N$ on the day $t \in T$ and the previous activity in the same city has been held on the day $t-s \in T$ $(l \le s \le t-1)$ by any politician, 0 otherwise
$S_{mit} \in \{0,1\}$	1 if politician $m \in M$ stays overnight in city $i \in N$ at the end of day $t \in T$, 0 otherwise
$V_{mt} \in \{0,1\}$	1 if politician $m \in M$ rests on day $t \in T$, 0 otherwise
$X_{mijt} \in \{0,1\}$	1 if arc $(i,j) \in A$ is traversed by politician $m \in M$ on day $t \in T$, 0 otherwise
$Z_{mit} \in \{0,1\}$	1 if politician $m \in M$ holds an activity in city $i \in N$ on day $t \in T$, 0 otherwise

each politician $m \in M$ has carried out at least p_{mk} activities in cities belonging to the cluster $k \in K$.

$$\sum_{m\in M}\sum_{t\in T} F_{mit} \le 1, \qquad \forall i \in N, \tag{6}$$

$$\sum_{m\in M} F_{mit} + \sum_{m\in M} Z_{miv} \le 1, \qquad \forall i \in N,\ \forall t, v \in T : 1 \le v \le t-1. \tag{7}$$

Constraints (6) guarantee that there can be at most one first activity held by any politician in each city. Constraints (7) link the variables F and Z, imposing that any city $i \in N$ cannot both host an activity for the first time on day $t \in T$ ($\sum_{m\in M} F_{mit} = 1$) and also other activities in the previous days ($\sum_{m\in M} Z_{miv} = 1$, $1 \le v \le t-1$).

$$Z_{mit} = F_{mit} + \sum_{l\le s\le t-1} R_{mits}, \qquad \forall m \in M,\ \forall i \in N,\ \forall t \in T, \tag{8}$$

$$R_{mits} \le \sum_{f\in M} Z_{fi(t-s)}, \qquad \forall m \in M,\ \forall i \in N,\ \forall t \in T,\ \forall s \in \mathbb{N} : l \le s \le t-1, \tag{9}$$

$$\sum_{f\in M}\sum_{v=t-s+1}^{t-1} Z_{fiv} \le \left\lceil \frac{s-1}{l} \right\rceil (1 - R_{mits}), \qquad \forall m \in M,\ \forall i \in N,\ \forall t \in T : l+1 \le t \le \bar{t},\ \forall s \in \mathbb{N} : l \le s \le t-1. \tag{10}$$

Constraints (8)–(10) ensure the consistency of the families of variables F, R, and Z. In particular, Constraints (8) ensure that whenever an activity is performed ($Z_{mit} = 1$), it must either be the first activity in that city ($F_{mit} = 1$) or follow a previous activity conducted by any politician on a day $t-s$ with s ranging from l up to $t-1$ ($\sum_{l\le s\le t-1} R_{mits} = 1$). Constraints (9) ensure that if politician $m \in M$ holds an activity in city $i \in N$ on day $t \in T$, and the previous activity in the same city has been carried out on day $t-s \in T$ ($R_{mits} = 1$), then someone has accomplished an activity on day $t-s$ in the same city ($\sum_{l\in M} Z_{li(t-s)} \ge 1$). Constraints (10) ensure that if $R_{mits} = 1$, then no activity can be carried out in city i by any politician between days $t-s+1$ and $t-1$ (included).

$$\sum_{i\in N} S_{mit} = 1, \qquad \forall m \in M,\ \forall t \in T, \tag{11}$$

$$\sum_{v=t}^{t+u-1} S_{m1v} \ge 1, \qquad \forall m \in M,\ \forall t \in T : 1 \le t \le \bar{t} - u + 1. \tag{12}$$

Constraints (11) make sure that each politician $m \in M$ on each day $t \in T$ has to stay overnight in a city $i \in N$. Constraints (12) ensure that each politician spends at least one night at the campaign center every $u \in \mathbb{N}^+$ consecutive days.

$$\sum_{v=t}^{t+g-1} V_{mv} \ge e, \qquad \forall m \in M,\ \forall t \in T : 1 \le t \le \bar{t} - g + 1, \tag{13}$$

$$Z_{mit} + V_{mt} \le 1, \qquad \forall m \in M,\ \forall i \in N,\ \forall t \in T, \tag{14}$$

$$\sum_{i\in N} Z_{mit} + V_{mt} \ge 1, \qquad \forall m \in M,\ \forall t \in T. \tag{15}$$

Constraints (13) guarantee that each politician is granted at least $e \in \mathbb{N}$ rest day every $g \in \mathbb{N}^+$ days, constraints (14) ensure that no activity is performed by a politician during its rest days and constraints (15) secure that each day is considered as a working or a rest day.

$$\sum_{i\in N} a_i Z_{mit} + \sum_{(i,j)\in A} d_{ij} X_{mijt} \le q, \qquad \forall m \in M,\ \forall t \in T, \tag{16}$$

$$\sum_{t\in T}\left(\sum_{i\in N} (h_i Z_{mit} + o_i S_{mit}) + \sum_{(i,j)\in A} c_{ij} X_{mijt}\right) \le b_m, \qquad \forall m \in M. \tag{17}$$

Resource limits are enforced by constraints (16) and (17): the former establishes that the daily tour of each politician plus the duration of the executed activities lasts no more than q hours, whereas the latter defines the spending limit for each politician by considering the costs associated with the traveling, the overnight stays and the activities organization.

$$\sum_{\substack{j\in N:\\(i,j)\in A}} X_{mijt} \le 1, \qquad \forall m\in M,\ \forall i\in N,\ \forall t\in T, \tag{18}$$

$$\sum_{\substack{j\in N:\\(j,i)\in A}} X_{mjit} \le 1, \qquad \forall m\in M,\ \forall i\in N,\ \forall t\in T, \tag{19}$$

$$\sum_{\substack{j\in N:\\(i,j)\in A}} X_{mijt} - \sum_{\substack{j\in N:\\(j,i)\in A}} X_{mjit} = L_{mit} - E_{mit}, \quad \forall m\in M,\ \forall i\in N,\ \forall t\in T. \tag{20}$$

Constraints (18)–(20) involve the family of variables X. First, constraints (18) and (19) ensure that each politician enters and leaves any node of the graph at most once per day. Next, constraints (20) impose that each politician both enters and leaves each city visited on any day, except for the first and last city when the politician travels along an open path (cf. the route of politician A on the first day in Fig. 1).

$$L_{mit} + E_{mit} \le 1, \qquad \forall m\in M,\ \forall i\in N,\ \forall t\in T, \tag{21}$$

$$\sum_{i\in N}(L_{mit} + E_{mit}) = 2J_{mt}, \qquad \forall m\in M,\ \forall t\in T, \tag{22}$$

$$E_{mit} \le S_{mit}, \qquad \forall m\in M,\ \forall i\in N,\ \forall t\in T, \tag{23}$$

$$S_{mit} \le S_{mi(t-1)} + E_{mit}, \qquad \forall m\in M,\ \forall i\in N,\ \forall t\in T, \tag{24}$$

$$L_{mit} \le S_{mi(t-1)}, \qquad \forall m\in M,\ \forall i\in N,\ \forall t\in T, \tag{25}$$

$$S_{mi(t-1)} \le L_{mit} + S_{mit}, \qquad \forall m\in M,\ \forall i\in N,\ \forall t\in T. \tag{26}$$

The effectiveness of (20) is due to constraints (21) imposing that at most one among variables E_{mit} and L_{mit} can be equal to one for each $m\in M$, $i\in N$ and $t\in T$ and to constraints (22) imposing that on any given day each politician must traverse a path which is either open or closed (open paths are characterized by the presence in the same day of exactly one node which is entered but not left, and exactly one node which is departed but not entered). Constraints (23)–(26) guarantee the consistency of the family of variables S with the families E and L, respectively. Constraints (23) impose that, if a politician enters a city without leaving it ($E_{mit} = 1$), then they must stay in that city for the night; whereas Constraints (24) ensure that if a politician spends the night in a city ($S_{mit} = 1$), then, on the previous day, they either spent the night in the same city or entered it at the end of an open path. Constraints (25) and (26) impose analogous restrictions for politicians leaving a city.

$$S_{mi(t-1)} \le \sum_{\substack{j\in N:\\(i,j)\in A}} X_{mijt} + S_{mit}, \qquad \forall m\in M,\ \forall i\in N,\ \forall t\in T, \tag{27}$$

$$Z_{mit} \le \sum_{\substack{j\in N:\\(i,j)\in A}} X_{mijt} + S_{mit}, \qquad \forall m\in M,\ \forall i\in N,\ \forall t\in T, \tag{28}$$

$$\sum_{\substack{j\in N:\\(j,i)\in A}} X_{mjit} \le Z_{mit} + S_{mit}, \qquad \forall m\in M,\ \forall i\in N,\ \forall t\in T. \tag{29}$$

Constraints (27) ensure the continuity of the path followed by each politician in consecutive days (cf. the starting city of politician B on the second and third day in Fig. 1), whereas constraints (28) impose that if a politician holds an activity in a city on any day, then it must visit that city on the same day. Constraints (29) make sure that, if a politician enters a city on a given day, then it holds an activity in that city and/or it spends the night there.

$$E_{mit},\ F_{mit},\ L_{mit},\ S_{mit},\ Z_{mit} \in \{0,1\}, \qquad \forall m\in M,\ \forall i\in N,\ \forall t\in T, \tag{30}$$

$$R_{mits} \in \{0,1\}, \qquad \forall m\in M,\ \forall i\in N,\ \forall t\in T,\ \forall s\in \mathbb{N}: l\le s\le t-1, \tag{31}$$

$$V_{mt} \in \{0,1\}, \qquad \forall m\in M,\ \forall t\in T, \tag{32}$$

$$X_{mijt} \in \{0,1\}, \qquad \forall m\in M,\ \forall (i,j)\in A,\ \forall t\in T. \tag{33}$$

Finally, constraints (30)–(33) define decision variables.

5. Excluding subtours

The mathematical model described so far satisfies all the requirements of the RM-PRP, except that it does not prevent closed subtours disconnected from the main route of each politician. In the following sections, we discuss three different strategies to exclude subtours.

5.1. Miller-Tucker-Zemlin constraints

As a first strategy to exclude subtours, we apply Miller-Tucker-Zemlin (MTZ) constraints [31] for the Traveling Salesman Problem (TSP): on a graph with n nodes, the formulation introduces $n-1$ continuous variables (one for each node except the depot) with value bounded between 2 and n, taking increasing values corresponding to the order in which nodes are visited, thus preventing subtours. In our problem, there are several key differences to consider to achieve a similar outcome: first, we have multiple routes (one for each politician on each day) rather than just one, and these routes can be open, closed, or even reduced to a single node (degenerate case). Moreover, only a subset of nodes is visited by each daily route. To adapt the MTZ technique to the RM-PRP, we introduce a continuous variable U_{mit} for each $m\in M$, $i\in N$, and $t\in T$. On each day $t\in T$, the variable U_{mit} will be set to 0 if politician m does not visit node $i\in N$, and it will be set to an increasing number greater than or equal to 1 otherwise, according to the order in which the politician visits the nodes. This is achieved with the addition of the following constraints:

$$U_{mit} \le \max\left\{1, \sum_{(j,u)\in A} X_{mjut} + J_{mt}\right\}, \qquad \forall m\in M,\ \forall i\in N,\ \forall t\in T, \tag{34}$$

$$U_{mit} \le (p+2)\left(\sum_{\substack{j\in N:\\(i,j)\in A}} X_{mijt} + S_{mit}\right), \qquad \forall m\in M,\ \forall i\in N,\ \forall t\in T, \tag{35}$$

$$U_{mit} \ge S_{mi(t-1)}, \qquad \forall m\in M,\ \forall i\in N,\ \forall t\in T, \tag{36}$$

$$U_{mit} \le (p+1)(1 - S_{mi(t-1)}) + 1, \qquad \forall m\in M,\ \forall i\in N,\ \forall t\in T, \tag{37}$$

$$U_{mit} \ge 2\sum_{\substack{j\in N:\\(j,i)\in A}} X_{mjit} - S_{mi(t-1)}, \qquad \forall m\in M,\ \forall i\in N,\ \forall t\in T, \tag{38}$$

$$(p+3)(S_{mj(t-1)} - X_{mijt} + 1) + U_{mjt} \ge U_{mit} + 1, \qquad \forall m\in M,\ \forall i,j\in N: i\ne j,\ \forall t\in T, \tag{39}$$

$$U_{mit} \ge 0, \qquad \forall m\in M,\ \forall i\in N,\ \forall t\in T. \tag{40}$$

For each politician $m\in M$ and each day $t\in T$, the right-hand side of constraints (34) bounds variable U_{mit} to be lower than or equal to the number of nodes visited by politician m on day t (including the node where they stopped on the previous day): this is equivalent to 1 in the degenerate case, equal to the number of traversed arcs in a closed path ($J_{mt} = 0$), and to the number of arcs plus one ($J_{mt} = 1$) in an open path. Notice that constraints (34) involve the 'max' operator, which can be linearized by introducing two 'big-M' constraints and a binary variable for each of the $\overline{m}\cdot\overline{n}\cdot\overline{t}$ constraints, significantly increasing the computational burden. To address this, we propose two alternatives. The first modifies (34) as follows:

$$U_{mit} \le \sum_{(j,u)\in A} X_{mjut} + J_{mt} + S_{mit(t-1)}, \qquad \forall m\in M,\ \forall i\in N,\ \forall t\in T. \tag{41}$$

For non-depot nodes, the constraint remains unchanged since $S_{mi(t-1)} = 0$, and the right-hand side is at least one. For depot nodes, the bound is one unit higher than necessary, but constraints (36) and (37) force $U_{mit} = 1$. The second option is as follows:

$$U_{mit} \le \sum_{\substack{(j,u)\in A:\\u\ne i}} X_{mjut} + J_{mt} + 1, \qquad \forall m\in M,\ \forall i\in N,\ \forall t\in T. \tag{42}$$

where we sum all traversed arcs except those entering city i. A manual verification confirms that the bound on U_{mit} is always sharp, except when i is the depot node of an open path and the bound results one unit higher than necessary, an issue fixed as already described above.

Constraints (35) force each variable U_{mit} to be zero when node $i \in N$ is not visited by politician m on day t. Otherwise, the constraints are not binding, as $p+2$ represents an upper bound on the number of nodes a politician can visit in a single day[8]). Constraints (36) and (37) ensure that U_{mit} is set to 1 when node i serves as the starting node of the path of politician m on the day t, while remaining non-binding otherwise. For each node $i \in N$ that belongs to a path and is not the depot, constraints (38) ensure that the variable U_{mit} takes a value of at least 2. These constraints are consistent with (35) when node i is not visited, and with (36) and (37) when i corresponds to the depot. Finally, constraints (39) are a modified version of the classical MTZ constraints. Whenever the arc $(i,j) \in A$ is not traversed by politician m on day t ($X_{mijt} = 0$), the constraint simplifies to:

$$(p+3)(S_{mj(t-1)} + 1) + U_{mjt} \geq U_{mit} + 1,$$

which always holds, as $p+3$ is a sharp upper bound for the right-hand side. Conversely, if the arc $(i,j) \in A$ is traversed ($X_{mijt} = 1$), the constraint becomes:

$$(p+3)S_{mj(t-1)} + U_{mjt} \geq U_{mit} + 1,$$

enforcing $U_{mjt} \geq U_{mit} + 1$ for each arc $(i,j) \in A$, except when j is the depot of a closed path ($S_{mj(t-1)} = 1$).

5.2. Subtour elimination constraints

An alternative approach to prevent subtours separated from a politician's route is to adapt the classical Subtour Elimination Constraints (SEC) proposed for the TSP (see [32]). Unlike the TSP, where each node is visited exactly once, in the RM-PRP a politician only traverses a subset of nodes each day. A closed path is allowed if and only if it includes the daily depot. To enforce this, for each proper subset $C \subset N$ containing at least two nodes, we have:

$$\sum_{(i,j)\in A(C)} X_{mijt} \leq |C| - 1 + \sum_{i\in C} S_{mit}, \qquad \forall m \in M,\ \forall t \in T,\ \forall C \subset N : |C| \geq 2, \tag{43}$$

where $A(C) = \{(i,j) \in A \mid i,j \in C\}$. Note that, whenever the daily depot belongs to set C, the right-hand side increases by 1 ($\sum_{i\in C} S_{mit} = 1$) and the constraint is no longer binding.

To solve an RM-PRP model with these constraints, a separation problem is used to dynamically add only violated ones. Following Pferschy and Staněk [33], we take advantage of modern MIP solvers by handling only integer solutions. Initially, SECs are omitted. Whenever a new integer solution is found, it is analyzed in polynomial time, and any detected subtour is eliminated by adding the corresponding constraint (43).

5.3. Connectivity constraints

Another approach to exclude subtours is to apply Connectivity Constraints (CC), which ensure a path from the depot to any target node by requiring at least one outgoing arc from any subset containing the depot but not the target. Given the exponential cardinality of CCs, they are dynamically added using row generation. Violated constraints are identified by solving the maximum flow problem between the depot and, in turn, each of the other nodes. Since a node can be visited both to hold an activity or as the final stop of a daily route, the revised CCs for the RM-PRP come in two families:

$$\sum_{(h,l)\in\delta^+(C)} X_{mhlt} \geq S_{mi(t-1)} + S_{mjt} - 1, \qquad \forall m \in M,\ \forall t \in T,\ \forall C \subset N : |C| \geq 1,\ \forall i \in C,\ \forall j \in N \setminus C, \tag{44}$$

$$\sum_{(h,l)\in\delta^+(C)} X_{mhlt} \geq S_{mi(t-1)} + Z_{mjt} - 1, \qquad \forall m \in M,\ \forall t \in T,\ \forall C \subset N : |C| \geq 1,\ \forall i \in C. \tag{45}$$

Let $C \subset N$ be a proper subset of nodes. For each politician $m \in M$ and each day $t \in T$, Constraints (44) is binding if and only if node $i \in C$ is the daily depot ($S_{mi(t-1)} = 1$, indicating that the politician stopped in node i at the end of day $t-1$) and node $j \in N \setminus C$ is visited as the last node of the daily path ($S_{mjt} = 1$). Similarly, the right hand side of constraints (45) is binding if and only if on day $t \in T$ a politician $m \in M$ both starts its daily path from node $i \in C$ ($S_{mi(t-1)} = 1$) and holds an activity in node $j \in N \setminus C$ ($Z_{mjt} = 1$). These constraints can be strengthened by observing that, for each politician $m \in M$ and each day $t \in T$, constraints (11) ensure that exactly one variable S_{mit} equals 1 among all $i \in N$, therefore the terms $S_{mi(t-1)}$ and S_{mjt} in the right-hand sides can be replaced by the sum of those variables over C and $N \setminus C$, respectively:

$$\sum_{(h,l)\in\delta^+(C)} X_{mhlt} \geq \sum_{i\in C} S_{mi(t-1)} + \sum_{j\in N\setminus C} S_{mjt} - 1, \qquad \forall m \in M,\ \forall t \in T,\ \forall C \subset N,\ |C| \geq 1, \tag{46}$$

$$\sum_{(h,l)\in\delta^+(C)} X_{mhlt} \geq \sum_{i\in C} S_{mi(t-1)} + Z_{mjt} - 1, \qquad \forall m \in M,\ \forall t \in T,\ \forall C \subset N : |C| \geq 1,\ \forall j \in N \setminus C. \tag{47}$$

In the following, we will refer to constraints (44) and (45) as the *base CCs* and to constraints (46) and (47) as the *strong CCs*. Since both involve an exponential number of inequalities, we dynamically identify the violated base CCs during the branch-and-bound process and add their strengthened counterparts to the MIP solver. Let

$$\overline{S} = \left(\{\overline{E}\}_{mit}, \{\overline{F}\}_{mit}, \{\overline{J}\}_{mt}, \{\overline{L}\}_{mit}, \{\overline{R}\}_{mits}, \{\overline{S}\}_{mit}, \{\overline{X}\}_{mit}, \{\overline{V}\}_{mt}, \{\overline{Z}\}_{mit}\right)$$

be the (possibly fractional) optimal solution of the continuous relaxation for a subproblem in the branch-and-bound solution tree. As each potential subtour belongs to the daily path of a given politician, we iterate over all politicians $m \in M$ and all days $t \in T$ to identify violated connectivity constraints. To this aim, we solve a maximum flow problem on a directed graph $\overline{G}_{mt} = (\overline{N}_{mt}, \overline{A}_{mt})$ with node set $\overline{N}_{mt} = \{\, i \in N \mid \overline{S}_{mi(t-1)} > 0 \vee \overline{S}_{mit} > 0 \vee \overline{Z}_{mit} > 0 \,\}$, arc set $\overline{A}_{mt} = \{\, (i,j) \in A \mid i,j \in \overline{N}_{mt} \,\}$ and arc capacity $\overline{X}_{mijt}$ for each $m \in M$, $t \in T$, and $(i,j) \in \overline{A}_{mt}$.

Algorithm 1 Connectivity constraints separation

```
1: function SeparateConnectivityConstraints(M, T, S̄)
2:   for all m ∈ M do
3:     for all t ∈ T do
4:       Ḡ_mt ← BuildPoliticianDailyGraph(S̄, m, t)
5:       for all i ∈ N̄'_mt do
6:         for all j ∈ N̄''_mt \ { i } do
7:           (C, f) ← MaxFlow(Ḡ_mt, i, j)
8:           if Σ_{i∈C} S_mi(t−1) + Σ_{l∈N̄_mt\C} S_mlt − 1 > f then
9:             AddConnectivityConstraint(46)(m, t, C)
10:          end if
11:          if Σ_{i∈C} S_mi(t−1) + Z_mjt − 1 > f then
12:            AddConnectivityConstraint(47)(m, t, C, j)
13:          end if
14:        end for
15:      end for
16:    end for
17:  end for
18: end function
```

Algorithm 1 describes the steps taken to determine violated constraints. At Lines 2 and 3, we loop through each politician $m \in M$ and each day $t \in T$. Then, at Line 4, we build the graph $\overline{G}_{mt}$ that takes into account only those nodes and arcs associated with non-zero variables in $\overline{S}$. Note that, for each fixed politician $m \in M$ and day $t \in T$, it is

[8] Indeed, whenever a politician visits a city, they must hold an activity, except at most for the starting and final city of their daily path.

enough to select the nodes $i \in N$ such that at least one variable among $S_{mi(t-1)}$, S_{mit} or Z_{mit} is non-zero. Indeed, constraints (8), (23), (25) and (29) ensure that whenever $S_{mi(t-1)}$, S_{mit} and Z_{mit} are zero, then E_{mit}, F_{mit}, L_{mit}, R_{mits}, X_{mijt} are zero for each $i, j \in N$ and each $l \leq s \leq t-1$. To separate violated constraints in (44) and (45) we are interested in finding the maximum flow on $\overline{G}_{mt}$ for each source–sink pair. To reduce the number of maximum flow problems to solve, we note that if any of the variables in the right-hand sides of (44) and (45) is zero, the associated inequality is surely satisfied. This allows to reduce the subset of source node to $\overline{N}'_{mt}$ and the subset of sink nodes to $\overline{N}''_{mt}$, where

$$\overline{N}'_{mt} = \left\{ i \in \overline{N}_{mt} \,\middle|\, \overline{S}_{mi(t-1)} > 0 \right\}, \qquad \forall m \in M,\ \forall t \in T,$$

$$\overline{N}''_{mt} = \left\{ i \in \overline{N}_{mt} \,\middle|\, \overline{S}_{mit} > 0 \ \vee\ \overline{Z}_{mit} > 0 \right\}, \qquad \forall m \in M,\ \forall t \in T.$$

At Lines 5 and 6 we loop through all possible source–sink pairs (i, j) and, at Line 7, we solve a max flow problem on $\overline{G}_{mt}$ from i to j using the Boykov–Kolmogorov algorithm for MaxFlow/MinCut [34]. Next, at Lines 8–10 we check if the associated constraint in (44) is violated; if so, we add its strengthened counterpart from constraints (46). At Lines 11–13 we do the same for constraints (45) and (47).

6. Valid inequalities

This section gathers a number of valid inequalities for the RM-PRP. These are cuts excluding fractional solutions from the feasible region of a mathematical model that already precludes subtours.

First, we observe that constraints (7) can be strengthened using constraints (3) as follow:

$$\sum_{m\in M} \sum_{t\leq u\leq \bar{t}} F_{miu} + \sum_{m\in M} \sum_{u=v}^{v+l-1} Z_{miu} \leq 1, \qquad \forall i \in N,\ \forall t, v \in T : 1 \leq v \leq t-l. \tag{7'}$$

Next, for each politician, each day, and city, the following relations hold:

$$L_{mit} + S_{mit} \leq 1, \qquad \forall m \in M,\ \forall i \in N,\ \forall t \in T, \tag{48}$$

$$E_{mit} + S_{mi(t-1)} \leq 1, \qquad \forall m \in M,\ \forall i \in N,\ \forall t \in T, \tag{49}$$

$$J_{mt} + S_{mi(t-1)} + S_{mit} \leq 2, \qquad \forall m \in M,\ \forall i \in N,\ \forall t \in T, \tag{50}$$

$$S_{mit} - S_{mi(t-1)} = E_{mit} - L_{mit}, \qquad \forall m \in M,\ \forall i \in N,\ \forall t \in T. \tag{51}$$

Constraints (48) exclude the possibility for a politician who travels on an open path starting in node i to stop in the same depot at the end of the same day. Similarly, constraints (49) impose that if node i is the arrival depot for an open path, the same node cannot be the depot for that politician on the day before. Constraints (50) make sure that, if a politician stays overnight in the same city on days t and $t-1$, then the path traveled on day t cannot be an open path and, conversely, if a politician travels along an open path, then it cannot stop in the same node on two consecutive days. Constraints (51) encode the consistency of E, L, and S variables on pairs of consecutive days.

Additionally, the following relations involving the family of variables X must be satisfied:

$$E_{mit} \leq \sum_{(j,i)\in A} X_{mjit}, \qquad \forall m \in M,\ \forall i \in N,\ \forall t \in T, \tag{52}$$

$$L_{mit} \leq \sum_{(i,j)\in A} X_{mijt}, \qquad \forall m \in M,\ \forall i \in N,\ \forall t \in T, \tag{53}$$

$$S_{mit} \leq \sum_{(j,i)\in A} X_{mjit} + S_{mi(t-1)}, \qquad \forall m \in M,\ \forall i \in N,\ \forall t \in T, \tag{54}$$

$$X_{mijt} + X_{mjit} \leq S_{mit} + S_{mjt} + 1, \qquad \forall m \in M,\ \forall (i,j) \in A,\ \forall t \in T. \tag{55}$$

Constraints (52) state that, if a city is entered as the final depot of a path, one of its incoming arcs must be active; and, similarly, constraints (53) impose that, if a city is the starting depot of an open path, one of its outgoing arcs must be selected. If node i is selected as the final depot by a politician m on day t, constraints (54) force the politician either to enter the node or already be there since the previous day. As fractional solutions having pairs of opposite arcs with non-zero values are quite common, constraints (55) impose that, whenever a politician travels along arc (i, j) and its reverse (j, i), then it must stay overnight on either i or j.

Regarding activities, the following constraints involving the families of variables F and Z must be met:

$$\sum_{(i,j)\in A} X_{mijt} \geq \sum_{i\in N} Z_{mit} - J_{mt}, \qquad \forall m \in M,\ \forall t \in T, \tag{56}$$

$$\sum_{(i,j)\in A} X_{mijt} \leq \sum_{i\in N} Z_{mit} + 1, \qquad \forall m \in M,\ \forall t \in T, \tag{57}$$

$$\sum_{f\in M} F_{fit} + \sum_{u=v}^{v+w-1} Z_{miu} \leq 1, \qquad \forall m \in M,\ \forall i \in N,\ \forall t, v \in T : 1 \leq v \leq t-w, \tag{58}$$

$$pV_{mt} + \sum_{i\in N} Z_{mit} \leq p, \qquad \forall m \in M,\ \forall t \in T. \tag{59}$$

As each politician takes an activity in each visited city except at most the first one and the last one of each daily route, constraints (56) and (57) provide upper and lower bounds on the number of arcs in a daily path by the number of activities performed on the same day. Also, the relation between variables F and Z can be further strengthened using constraints (58). Constraints (59) do the same for variables V and Z. Moreover, the following inequalities involving the variables R can be added:

$$\sum_{\substack{m\in M\\ t\leq v\leq \bar{t}\\ \max(v-t+1,l)\leq s\leq v-1}} R_{mivs} + \sum_{m\in M} F_{mit} \leq 1, \qquad \forall i \in N,\ \forall t \in T, \tag{60}$$

$$\sum_{\substack{m\in M\\ t+1\leq v\leq \bar{t}\\ \max(v-t+1,l)\leq s\leq v-1}} R_{mivs} + \sum_{m\in M} Z_{mit} \leq 1, \qquad \forall i \in N,\ \forall t \in T, \tag{61}$$

$$Z_{mit} + \sum_{f\in M} Z_{fi(t-s)} - \sum_{f\in M} \sum_{v=t-s+1}^{t-1} Z_{fiv} - 1 \leq R_{mits}, \qquad \forall m \in M,\ \forall i \in N,\ \forall t \in T,\ \forall s \in \mathbb{N} : l \leq s \leq t-1. \tag{62}$$

Constraints (60) and constraints (61) impose that, if politician $m \in M$ holds an activity in city $i \in N$ on day $t \in T$ (i.e. $F_{mit} = 1$ or $Z_{mit} = 1$), then variables R_{mivs} $(v - s + 1 \leq t \leq v - 1)$ are forced to zero, and, conversely, if any of those variables is set to one, then all the others (including F_{mit} and Z_{mit}) must be 0. Fixing the index $t \in T$ of R_{mits} (rather than the index t of Z_{mit} as in the previous inequalities) and allowing the index t of Z_{mit} to vary, we obtain constraints (62).

Finally, the following cuts encode the fact that, if a politician starts ($S_{mi(t-1)} = 1$) or terminates ($S_{mit} = 1$) their daily route in node $i \in N$ and traverses any arc $(j, k) \in A$ not starting/ending in i, then they must leave/enter node i, respectively:

$$S_{mi(t-1)} + X_{mjkt} - 1 \leq \sum_{(i,v)\in A} X_{mivt}, \qquad \forall m \in M,\ \forall (j,k) \in A,\ \forall i \in N \setminus \{ j \},\ \forall t \in T, \tag{63}$$

$$S_{mit} + X_{mjkt} - 1 \leq \sum_{(v,i)\in A} X_{mvit}, \qquad \forall m \in M,\ \forall (j,k) \in A,\ \forall i \in N \setminus \{ k \},\ \forall t \in T. \tag{64}$$

7. Sequential route construction matheuristic

As discussed in Section 2, the RM-PRP is NP-hard, which implies that solving large-size instances is computationally challenging. For this reason, we develop a Sequential Route Construction Matheuristic (SRCM) to build a high-quality solution exploiting the multi-period nature of the RM-PRP. The idea in SRCM is to solve a sequence of sub-problems, each one devoted to identify the most convenient route for each politician on a single day. When doing so, a number of constraints

Algorithm 2 Sequential Route Construction Matheuristic (SRCM)

1: **function** BuildSrcmSolution(RM-PRP instance)
2: $\tilde{\tau}_i \leftarrow -l, \quad \forall i \in N$ ▷ Day of the most recent activity in city i
3: $\tilde{\sigma}_m \leftarrow 1, \quad \forall m \in M$ ▷ Last city visited by politician m
4: $\tilde{b}_m \leftarrow b_m, \quad \forall m \in M$ ▷ Remaining budget for politician m
5: $\tilde{\rho}_{mi} \leftarrow -w, \quad \forall m \in M,\ \forall i \in N$ ▷ Day of the most recent activity in city i by politician m
6: $\tilde{p}_{mk} \leftarrow p_{mk}, \quad \forall m \in M,\ \forall k \in K$ ▷ Remaining minimum number of activities in cluster k by m

7: $\Delta_t \leftarrow \sum_{m \in M, i \in I} r_{mit}, \quad \forall t \in T,$
8: $\tilde{\Gamma} \leftarrow$ FindMinimalSubset$(1, u, \Delta)$ ▷ Subset of days chosen to rest at the campaign center
9: $\tilde{\Omega} \leftarrow$ FindMinimalSubset(e, g, Δ) ▷ Subset of days chosen as rest days

10: $\mathcal{S} \leftarrow \emptyset$
11: **for all** $t \in T$ **do**
12: $\sigma'_m \leftarrow \tilde{\sigma}_m, \quad \forall m \in M$
13: $\gamma'_m \leftarrow (t \in \tilde{\Gamma})$? *true* : *false*, $\quad \forall m \in M$
14: $b'_m \leftarrow \tilde{b}_m / (\bar{t} - t + 1), \quad \forall m \in M$
15: $r'_{mi} \leftarrow (\tilde{\tau}_i = 0)$? r_{mit} : $r'_{mit(t-\tilde{\tau}_i)}, \quad \forall m \in M,\ \forall i \in N$

16: **for** $m \in M$ **do**
17: $\lambda'_m = \{ i \in N \mid t \geq \tilde{\tau}_i + l,\ t \geq \tilde{\rho}_{mi} + w \}$ ▷ Cities available for the politician m on day t
18: $k' \leftarrow$ EnforceFeasibility$(\tilde{p}_{mk}, \tilde{\Omega}, \tilde{\Gamma})$ ▷ Cluster for potential constrained activity on day t
19: **if** $k' \neq$ **null then**
20: $p'_{mk'} \leftarrow 1$
21: **end if**
22: **end for**

23: **if** $t \notin \tilde{\Omega}$ **then**
24: $\mathcal{D} \leftarrow$ SolveDailyModel$(b', \lambda', \sigma', \gamma', r', p')$
25: **else if** $t \in \tilde{\Gamma}$ **then**
26: $\mathfrak{S} \leftarrow$ TravelToCampaignCenterAndStay()
27: **else**
28: $\mathfrak{S} \leftarrow$ StayAtCurrentCity()
29: **end if**

30: AppendDailyRoutes$(\mathcal{S}, \mathcal{D})$
31: UpdateQuantities$(\mathcal{D}, \tilde{b}, \tilde{\tau}, \tilde{\rho}, \tilde{\sigma}, \tilde{p})$
32: **end for**

33: **return** $\mathcal{S}$
34: **end function**

and decisions that were originally integrated into the formulation of the original (global) MILP model (such as rest days, overnight stays at the campaign center, etc.), must now be handled externally by a procedure that takes care to build and solve the subproblems in such a way that all original RM-PRP requirements are satisfied in the final solution.

The function BuildSrcmSolution in Algorithm 2 describes the procedure we adopt to build a solution for an RM-PRP instance. The quantities involved in this procedure fall mainly into two categories: those referring to global quantities that increase/decrease moving from one day to the next one will be marked by a tilde (˜), whereas the values of the parameters used to build the model for a single day will be marked by an apex (′).

At Line 2, we initialize to 0 the variables $\tilde{\tau}_i$ that hold the day of the most recent activity in city $i \in N$ and, at Line 3, we initially record the campaign center in the variables $\tilde{\sigma}_m$ that hold the daily depot of the politician $m \in M$ (as each politician is required to start their route from the campaign center). At Line 4, the remaining budget $\tilde{b}_m$ of each politician is set equal to their total budget b_m and, at Line 5, for each city $i \in N$, the day $\tilde{\rho}_{mi}$ of its most recent activity in city i is set to 0. As no activity has been scheduled so far, at Line 6, the variables $\tilde{p}_{mk}$ tracking the remaining number of required activities in each cluster $k \in K$ are set equal to the parameters p_{mk} of the instance. Before solving the restricted subproblems, at Lines 8–9 we choose upfront the subset $\tilde{\Gamma} \subseteq T$ of days in which politicians will spend the night in the campaign center and the subset $\tilde{\Omega} \subseteq T$ of days in which all politicians will rest. Both these subsets are computed through the function FindMinimalSubset(a, b, Δ) where a and b are non-negative integers with $a \leq b$ (1 and u, and e and g, respectively) and Δ is the set of $\bar{t}$ values computed at Line 7 that represents the total first activity rewards computed with respect to all politicians and cities for each day in the planning horizon. The goal of the function FindMinimalSubset is to identify a pattern $\Pi \subseteq T$ containing exactly a consecutive days every b days that minimizes the value of $\sum_{t \in \Pi} \Delta_t$ (such a pattern can be found in polynomial time through a complete enumeration of the search space).

We now solve a sequence of subproblems, each associated with a single day in T. At Line 10 we initialize an empty solution for the RM-PRP instance which will be incrementally built. Next, at Lines 11–32, the algorithm loops through each day in the planning horizon with the goal of solving a restricted problem for each of them. Before building these models, we must compute their parameters in such a way that the concatenation of the routes followed by each politician across all days provides a feasible solution for the RM-PRP instance at hand. To this aim, at Line 12 we set the starting city of each politician $m \in M$ equal to the city where they stopped in the previous day/iteration. At Line 13, we check if the current day belongs to the subset of days chosen to rest in the campaign center, and, if so, we set the γ'_m variables to ***true***. Also, at Line 14, we assign to each politician a daily budget equal to their remaining total $\tilde{b}_m$ divided by the remaining number of days and, at Line 15, we compute the daily reward r'_{mi} for each pair of politician $m \in M$ and city $i \in N$ according to the latest activity held in i.

At lines 16–22, for each politician $m \in M$, first we compute the subset of cities where they can hold an activity on the current day (i.e. those respecting the restrictions imposed by the RM-PRP parameters l and w) and, then, we ensure that the minimum number of activities required in each cluster will be satisfied in the final (global) solution. To this end, in function EnforceFeasibility, we check if the total number of required activities left in clusters equals the number of remaining working days when the politician is not forced to stop at the campaign center. If this is the case, the function selects one cluster k' among those with unsatisfied activities and we set the corresponding variable $p'_{mk'}$ to 1 to force an activity inside such cluster during the daily route. At Lines 23–29 we are now ready to compute the daily routes for each politician. If the current day $t \in T$ does not belong to the set $\tilde{\Omega}$ of rest days, we build a single-day model using the parameters $(b', \lambda', \sigma', \gamma', r', p')$ computed so far and we let the MILP solver find the optimal solution. Otherwise, if $t \in \tilde{\Omega}$, we manually build a simple solution in which the politician either stays in their current city or travels to the campaign center and stops there (if $t \in \tilde{\Gamma}$). At line 30 we extend the RM-PRP solution $\mathcal{S}$ with the daily solution $\mathcal{D}$ built for the current day and, at Line 31, we update the global quantities (marked by ˜) accounting for the resources used in the daily solution $\mathcal{D}$. Finally, at Line 33, we return the solution for the RM-PRP instance.

8. Computational study

This section presents the results of computational experiments aimed at evaluating the efficacy of the developed matheuristic, alongside the contribution of the approaches employed to strengthen the original formulation. The experiments were executed on a machine equipped with an AMD Ryzen 9 3950X CPU (2.30 GHz) with 16 physical cores and 32 logical cores paired with 32 GB of RAM running Ubuntu Linux 22.04.3 LTS in a virtual machine. The algorithms were implemented in Java 21 and the mixed integer linear programming models were solved with Gurobi 11.0.3 using a time limit of 3 h.

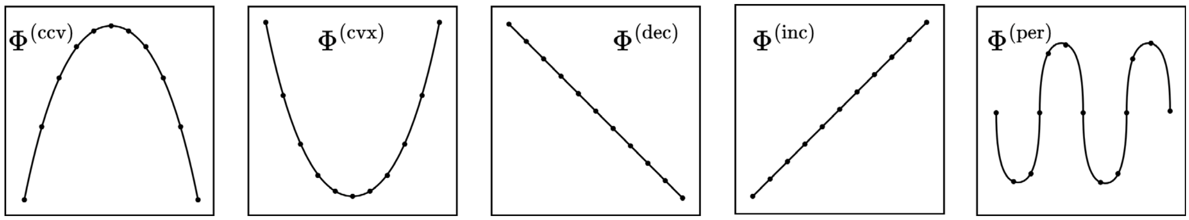

Fig. 2. Reward profiles $\Phi^{(\cdot)}$ considered for the RM-PRP.

This paper is the first to introduce the RM-PRP. We generate benchmark instances based on real data from the US presidential elections as explained in Appendix. Since we consider as locations the capitals of each US state plus the District of Columbia, in this section we will use the terms *node*, *city* and *state* interchangeably to ease the exposition. Instance names follow the convention *US_[politicians]_[states]_[days]_[clusters]* providing comprehensive information about their characteristics, e.g. instance *US_m2_s51_t40_c3* pertains to the US elections (*US*), contains 2 politicians (*m2*), 50 states plus the District of Columbia (*s51*), 40 days (*t40*), and 3 clusters of states (*c3*). Instances were generated by varying the number of politicians (ranging from 1 to 3), the number of days (5, 10, 15, 20, 30, and 40), and the number of clusters (3 and 4), resulting in $3 \cdot 6 \cdot 2 = 36$ instances. The data used to generate the instances are publicly accessible at https://github.com/lmores/or-rmprp-data.

In Section 8.1 we explain how reward values were generated. The performance of the various developed formulations is compared in Section 8.2, where we also analyze the benefits of incorporating connectivity constraints. Section 8.3 evaluates the five reward trends, followed by an assessment of the efficiency and effectiveness of the developed matheuristic in Section 8.4. Section 8.5 reports cut violations, and finally, Section 8.6 presents sensitivity analysis results.

8.1. Reward values

In the model formulation (Section 4), the reward functions Φ and Φ' are left undefined to allow for modeling flexibility to represent different plausible campaign dynamics and voter engagement trends over time. In this section, we specify the concrete reward profiles Φ used in our computational experiments and accordingly define the function $\Phi'(t,s) = \Phi(t) \cdot \phi(s)$ where $\phi(s)$ is a penalization function applied to the reward and based on the number of days $s \in \mathbb{N}^+$ elapsed since the previous activity in the same city. It is designed to assign a stronger penalty to closely spaced visits, while progressively reducing its effect as s increases. The rationale is to preserve the temporal logic encoded by Φ while penalizing short-term repetition. In particular, we decided to set $\phi(s) = {}^{s}/_{\bar{t}}$ which works as a penalty that progressively vanishes as s increases ($\bar{t}$ being the size of the planning horizon), reflecting the idea that revisiting a city becomes more valuable the longer the gap since the last visit.

While the political science literature provides limited consensus on how campaign impact evolves over time, several interpretations are commonly considered. Some models assume that campaign effectiveness decreases as the election approaches [17], while others suggest the opposite [35]. Still, others advocate for non-monotonic trends, such as "U-shaped" curves, or emphasize the strategic value of early visibility for fundraising and local mobilization. A widely accepted idea, however, is that candidates tend to intensify their efforts near the end of the race, concentrating activities in key locations [36].

To reflect this variety of strategic visions where $r_{mit} = \tilde{r}_{mi}\Phi(t)$, we tested five distinct temporal profiles for Φ, each capturing a different reward logic. Given parameters $\alpha, \gamma, \delta, \omega \in \mathbb{R}^+$ and $\beta \in \mathbb{R}$, we define:

$$\Phi_t^{(\mathrm{ccv})} = -\alpha\left(t - \frac{\bar{t}+1}{2}\right)^2 + \beta, \qquad \Phi_t^{(\mathrm{cvx})} = \alpha\left(t - \frac{\bar{t}+1}{2}\right)^2 + \beta,$$

$$\Phi_t^{(\mathrm{dec})} = 1 - \frac{t}{\bar{t}}, \qquad \Phi_t^{(\mathrm{inc})} = \frac{t}{\bar{t}}, \qquad \Phi_t^{(\mathrm{per})} = \gamma\,(1 - \delta\sin(\omega t)),$$

namely, non-linear concave ($\Phi^{(\mathrm{ccv})}$), non-linear convex ($\Phi^{(\mathrm{cvx})}$), linearly decreasing ($\Phi^{(\mathrm{dec})}$), linearly increasing ($\Phi^{(\mathrm{inc})}$), and periodic ($\Phi^{(\mathrm{per})}$). These profiles are illustrated in Fig. 2. They allow us to explore how different temporal reward dynamics affect optimal campaign planning in the RM-PRP. The following parameter values were used in our tests: $\alpha = 0.002358$, $\beta = \gamma = \delta = \frac{1}{2}$ and $\omega = \frac{2\pi}{5}$.

Finally, we mention that all reward values (r_{mit} and r'_{mits}) computed as above have been truncated to their integer part before using them as coefficients in the objective function to avoid rounding errors when comparing the value of different feasible solutions.

8.2. Performance comparison of alternative formulations for subtours elimination

In this section, we solve US instances alternatively using MTZ, SEC, and CC constraints. To run computational experiments throughout this section, we replace (34) with (42) as they involve fewer variables than (41) and, therefore, are less prone to numerical instability issues. In this set of experiments, we employ $\Phi^{(\mathrm{cvx})}$ to compute the reward values. We start by directly comparing the MTZ and SEC formulations instance by instance. The comparison results are illustrated in Fig. 3, where the bars represent the objective function values of the two formulations (left vertical axis), whereas the line charts (values on the right vertical axis) report the corresponding MipGap values reached by Gurobi when reaching the 3-hour limit. Detailed figures and average values are shown in columns three to six of Table 3.

Although SEC-based formulations are known to provide tighter linear relaxations than MTZ in theory, this advantage is not fully reflected in our experimental results. Among the 23 instances where both formulations find a feasible solution, the MTZ model significantly outperforms the SEC formulation, achieving an average optimality gap of 46.21%, compared to 80.84% for the SEC model. This is mainly due to the lazy constraint strategy adopted for SECs, which delays their addition until an integer solution is found. As a consequence, the MTZ model, which is fully loaded from the beginning, often benefits from a more constrained search space early on, especially for larger instances. Nonetheless, on smaller instances ($\bar{t} = 5$), the SEC formulation demonstrates competitive performance despite its initial disadvantage. In this setting, it achieves a lower average MIP gap (6.8%) compared to MTZ (12.3%), indicating that the SEC approach can be effective when the instance size allows timely generation of subtour elimination constraints. While pre-loading some short-cycle SECs (e.g., 2- and 3-cycles) could potentially strengthen the initial formulation, preliminary tests revealed a considerable increase in computational time without consistent benefits in solution quality. For this reason, we chose to adopt a lazy constraint strategy throughout the experimental campaign.

The average objective value in these 23 instances was 62,576 for the model using MTZ constraints, substantially exceeding the 53,848 obtained by the formulation with SEC constraints. Furthermore, in nine instances where the model with SEC constraints failed to find a feasible solution within 3 h of CPU time, the MTZ formulation successfully obtained one. However, it is important to note that SEC constraints are

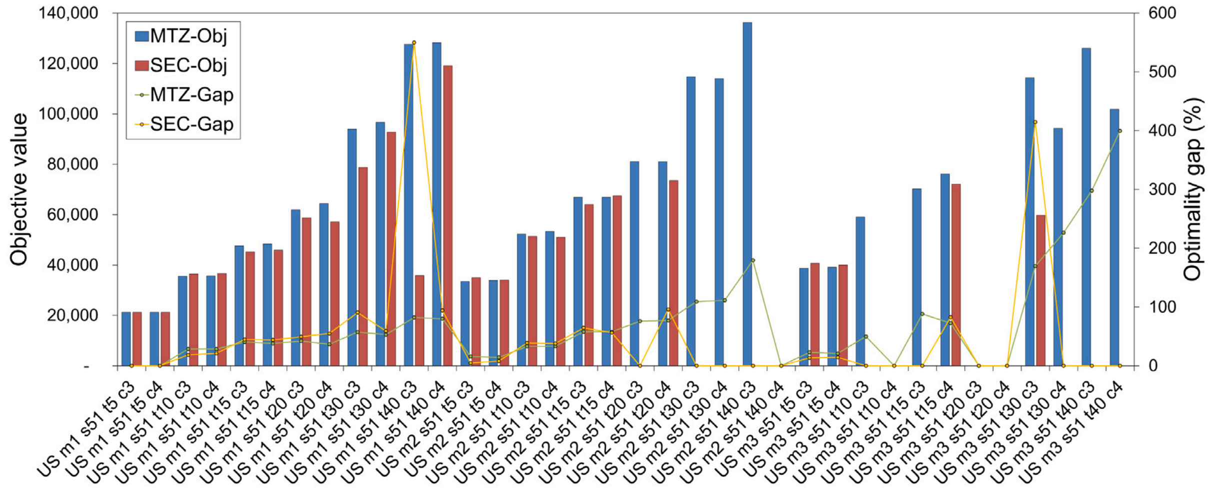

Fig. 3. Comparison of MTZ and SEC formulations using the convex reward profile ($\Phi^{(\mathrm{cvx})}$).

Table 3
Comparison of solutions obtained using SRCM, the original model, and tightened models.

	$\Phi^{(\mathrm{cvx})}$								
Instance	SRCM	MTZ		SEC		CC+MTZ		CC+SEC	
	Obj	Obj	Gap	Obj	Gap	Obj	Gap	Obj	Gap
US_m1_s51_t5_c3	19 201	**21 260**	0.0%	**21 260**	0.0%	**21 260**	0.0%	**21 260**	0.0%
US_m1_s51_t5_c4	18 318	**21 260**	0.0%	**21 260**	0.0%	**21 260**	0.0%	**21 260**	0.0%
US_m1_s51_t10_c3	27 912	35 603	28.5%	**36 424**	18.6%	35 224	22.5%	36 340	8.4%
US_m1_s51_t10_c4	27 550	35 711	28.5%	**36 640**	21.2%	36 362	18.3%	**36 640**	3.4%
US_m1_s51_t15_c3	36 881	47 624	40.6%	45 278	44.9%	48 281	36.4%	**49 086**	28.9%
US_m1_s51_t15_c4	36 881	48 401	38.1%	45 940	43.9%	**49 236**	31.0%	49 111	29.6%
US_m1_s51_t20_c3	47 397	61 945	42.2%	58 751	49.3%	61 703	44.0%	**62 173**	40.8%
US_m1_s51_t20_c4	47 397	**64 436**	36.7%	57 152	55.0%	62 116	43.2%	61 990	40.8%
US_m1_s51_t30_c3	73 773	94 017	57.4%	78 773	90.6%	**95 086**	56.8%	87 655	67.9%
US_m1_s51_t30_c4	73 773	**96 650**	53.1%	92 756	59.3%	90 684	61.5%	85 309	69.5%
US_m1_s51_t40_c3	105 230	127 626	82.2%	35 811	550.0%	**128 591**	76.1%	106 761	106.4%
US_m1_s51_t40_c4	105 230	128 265	80.2%	119 108	94.1%	**133 573**	74.3%	105 633	120.1%
US_m2_s51_t5_c3	29 421	33 546	15.9%	**35 010**	4.8%	**35 010**	2.7%	**35 010**	0.0%
US_m2_s51_t5_c4	28 471	33 957	14.3%	34 087	8.1%	34 231	7.1%	**34 514**	2.7%
US_m2_s51_t10_c3	42 692	52 309	33.1%	51 413	39.1%	52 740	34.4%	**54 065**	30.8%
US_m2_s51_t10_c4	42 411	**53 388**	33.3%	51 031	38.0%	53 284	34.3%	52 848	31.1%
US_m2_s51_t15_c3	53 697	66 918	57.9%	64 019	64.6%	**67 169**	55.7%	66 133	59.4%
US_m2_s51_t15_c4	53 697	66 949	57.9%	**67 534**	56.5%	67 309	54.8%	63 557	64.0%
US_m2_s51_t20_c3	66 586	**81 101**	76.0%	–	–	79 859	80.5%	79 192	81.3%
US_m2_s51_t20_c4	66 586	**81 076**	77.1%	73 610	95.9%	78 103	83.5%	77 647	85.6%
US_m2_s51_t30_c3	100 187	114 723	109.1%	–	–	**119 521**	99.8%	107 477	122.9%
US_m2_s51_t30_c4	100 187	113 985	111.4%	–	–	**119 923**	99.8%	102 492	135.2%
US_m2_s51_t40_c3	138 842	136 327	179.6%	–	–	**154 606**	146.2%	141 223	168.2%
US_m2_s51_t40_c4	138 842	–	–	–	–	**153 466**	146.7%	142 076	168.8%
US_m3_s51_t5_c3	34 593	38 712	22.9%	40 696	13.5%	40 589	14.5%	**40 772**	10.7%
US_m3_s51_t5_c4	33 490	39 098	20.9%	**40 046**	14.4%	39 418	17.4%	39 810	13.6%
US_m3_s51_t10_c3	50 153	59 097	49.8%	–	–	**60 590**	45.9%	55 693	58.7%
US_m3_s51_t10_c4	51 139	–	–	–	–	59 042	48.3%	**59 271**	48.8%
US_m3_s51_t15_c3	61 569	70 185	88.2%	–	–	**73 583**	75.6%	68 399	89.0%
US_m3_s51_t15_c4	61 527	**76 148**	72.5%	72 121	82.7%	72 439	78.3%	69 783	85.3%
US_m3_s51_t20_c3	74 740	–	–	–	–	**89 480**	96.2%	78 438	124.5%
US_m3_s51_t20_c4	74 740	–	–	–	–	**85 626**	105.9%	74 873	136.2%
US_m3_s51_t30_c3	104 868	**114 361**	169.6%	59 795	414.8%	108 872	177.7%	107 007	181.3%
US_m3_s51_t30_c4	104 868	94 259	226.3%	–	–	**113 844**	165.0%	106 046	183.1%
US_m3_s51_t40_c3	147 624	126 050	298.0%	–	–	**155 799**	221.6%	150 090	222.7%
US_m3_s51_t40_c4	147 624	101 846	399.7%	–	–	**149 464**	235.4%	149 134	223.4%
Avg	**67 447.1**	**73 026.0**	**81.3%**	**53 848.5**	**80.8%**	**79 092.9**	**72.0%**	**74 410.2**	**79.0%**

applied only to integer solutions with subtours found by Gurobi in the branch-and-bound tree. In smaller instances with a single politician, the average number of integer solutions is 12 (with a minimum of 7 and a maximum of 22). In larger instances with three politicians, the

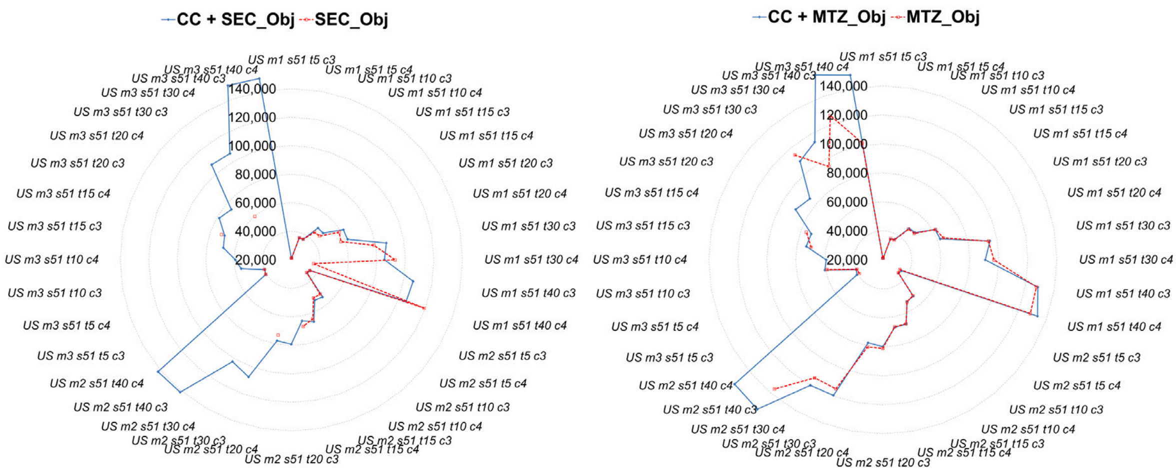

Fig. 4. Objective values of MTZ and SEC formulations with CC using the convex reward profile ($\Phi^{(cvx)}$).

average number of integer solutions drops to 5.5, with a minimum of zero (which helps explain the absence of feasible solutions in some cases) and a maximum of 17.

Key Observation 1: *The model with MTZ constraints leads to a better average performance than the formulation with SECs. Two interrelated reasons explain this result. First, MTZ constraints eliminate subtours a priori, reducing the search space and enabling Gurobi's primal heuristics to operate more effectively. Second, SECs are only enforced through lazy constraints, allowing infeasible solutions containing substours to persist longer during the search. This is supported by the solver logs, which show that the MTZ model produces significantly more successful heuristic improvements than SEC (195 vs 143 with one politician, 221 vs 128 with two, and 124 vs 57 with three).*

In the following, we verify the effect of adding connectivity constraints (CC), strengthening the model with valid inequalities and warm-starting the solver. In particular, we define CC+MTZ as the model obtained by replacing Constraint (7) with (7'), incorporating the MTZ constraints, dynamically enforcing the connectivity constraints as described in Section 5.3, and dynamically loading the violated valid inequalities presented in Section 6. In particular, connectivity constraints are checked every 100 nodes, and the most violated one for each politician is added if its violation exceeds 0.01. Analogously, the model CC+SEC corresponds to the same setup with MTZ constraints replaced by SEC applied dynamically on integer solutions. Finally, the rationale for providing a feasible solution as a warm start lies in its potential to improve MILP solver performance, as many state-of-the-art solver procedures require an initial feasible solution. While these solvers can efficiently find feasible solutions for problem instances with a limited number of days, their performance significantly declines as the planning horizon grows.

In Fig. 4, the radar charts on the left and right depict the results obtained by embedding CCs and warm-starting the formulations with SEC and MTZ constraints, respectively. Detailed and average results are provided in the last four columns of Table 3. The introduction of CCs combined with warm-starting the solver using SRCM solutions significantly tightens the formulations. The average optimality gaps are reduced from 81.3% to 72% for the formulation with MTZ constraints and from 80.84% to 79% for that with SEC constraints. In particular, for the instance *US_m2_s51_t5_c3*, the addition of connectivity constraints results in obtaining the optimal solution, not reached before. Moreover, a consistent pattern seems to emerge: as size of the instances increases, the performance of lazy constraints of SEC formulation deteriorates. Specifically, when comparing the three groups of instances with 1, 2, and 3 politicians, we observe that for smaller instances (with fewer days), the separation of SEC constraints yields smaller optimality gaps. However, as the number of days increases, formulation with MTZ constraints achieves smaller gaps. This suggests that, also in the presence of a tighter formulation with connectivity constraints, the model with SEC constraints becomes less effective as the size of the instances grows. However, in instances with one, two, and three politicians, the combination of CC+SEC constraints leads to 6, 3, and 3 best-known values, respectively.

Key Observation 2: *As the instance size (and difficulty) increases, the performance of the model with lazy SEC constraints deteriorates, although combined with CCs the formulation allows us to get 10 best-known values of which 3 are also optimal. For larger instances with more days, the model with MTZ and CC constraints achieves smaller optimality gaps and obtains 19 best-known values overall, including 2 optimal solutions.*

8.3. Comparison of different reward profiles

As discussed in Section 3, the decision-making processes in political election campaigns remain unclear, with limited empirical research in political science. Therefore, we explore a comprehensive range of 5 potential models that a decision-maker might adopt: $\Phi^{(ccv)}$ represents an inverse U-shape, where rewards are lower at both the start and end of the campaign, but peak in the middle; $\Phi^{(cvx)}$ suggests a U-shaped pattern where rewards are higher at the beginning and end of the campaign, with a decline in the middle; $\Phi^{(dec)}$ assumes rewards are higher at the start of the campaign and decrease linearly over time; $\Phi^{(inc)}$ establishes rewards are initially lower but increase linearly as the campaign progresses toward its conclusion; $\Phi^{(per)}$ function describes a scenario in which rewards fluctuate periodically.

Table 4 compares the best solutions found by formulation CC+SEC when each reward profile is selected. The reward profile $\Phi^{(dec)}$ that prioritizes early activities in the planning horizon generally demonstrates smaller optimality gaps (31.9% on average) than the other reward types in most instances. Intuitively, this is in line with the fact that only the starting city of each politician is set a priori, and this probably allows the solver to easily identify the optimal choices for the values of variables associated with the first days of the planning horizon. In contrast, the model using the reward profile $\Phi^{(inc)}$ performs the least favorably by exhibiting the highest average optimality gap (59.9%) among the five functions, and the models that embed the reward profiles $\Phi^{(cvx)}$ and $\Phi^{(ccv)}$ achieve only three optimal solutions while the other reward profiles obtain six optimal solutions. The periodic reward function, on the other hand, produces the second-lowest average optimality gap (40.6%).

Key Observation 3: *The model including linearly decreasing rewards proves to be the easiest to solve, while linearly increasing rewards are the*

Table 4
Comparison of reward profiles.

Instance	$\Phi^{(ccv)}$			$\Phi^{(cvx)}$			$\Phi^{(dec)}$			$\Phi^{(inc)}$			$\Phi^{(per)}$		
	SRCM	Obj	Gap	SRCM	Obj	Gap	SRCM	Obj	Gap	SRCM	Obj	Gap	SRCM	Obj	Gap
US_m1_s51_t5_c3	18 861	20 896	0.0%	19 201	21 260	0.0%	24 906	27 952	0.0%	20 773	28 547	0.0%	20 745	22 630	0.0%
US_m1_s51_t5_c4	18 011	20 896	0.0%	18 318	21 260	0.0%	24 560	27 952	0.0%	19 040	28 547	0.0%	20 290	22 630	0.0%
US_m1_s51_t10_c3	25 746	32 814	8.1%	27 912	36 340	8.4%	32 512	40 242	0.0%	28 633	40 355	0.0%	28 940	37 548	0.0%
US_m1_s51_t10_c4	24 962	32 982	6.2%	27 550	36 640	3.4%	31 029	40 242	0.0%	26 900	40 355	0.0%	28 660	37 548	0.0%
US_m1_s51_t15_c3	29 634	38 942	34.0%	36 881	49 086	28.9%	42 629	49 653	30.9%	34 768	48 931	27.2%	35 129	49 301	23.2%
US_m1_s51_t15_c4	29 634	38 466	35.5%	36 881	49 111	29.6%	42 629	50 247	28.8%	34 768	47 887	31.0%	35 129	50 234	20.3%
US_m1_s51_t20_c3	34 499	40 423	46.7%	47 397	62 173	40.8%	49 022	58 503	40.2%	39 655	56 723	37.9%	42 548	60 267	29.2%
US_m1_s51_t20_c4	34 499	39 305	48.2%	47 397	61 990	40.8%	49 022	56 635	45.2%	39 655	57 600	35.8%	42 548	59 639	30.8%
Avg	**26 981**	**33 090**	**22.3%**	**32 692**	**42 232**	**19.0%**	**37 039**	**43 928**	**18.1%**	**30 524**	**43 618**	**16.5%**	**31 749**	**42 475**	**12.9%**
US_m2_s51_t5_c3	28 874	34 226	0.0%	29 421	35 010	0.0%	35 529	44 191	0.0%	34 434	45 559	0.0%	29 729	36 193	0.0%
US_m2_s51_t5_c4	27 958	33 908	2.7%	28 471	34 514	2.7%	35 156	44 191	0.0%	32 568	44 900	0.0%	29 240	36 193	0.0%
US_m2_s51_t10_c3	39 738	48 115	34.8%	42 692	54 065	30.8%	51 265	59 699	30.8%	41 268	59 531	32.9%	44 248	56 820	22.4%
US_m2_s51_t10_c4	38 725	49 399	32.2%	42 411	52 848	31.1%	51 265	59 879	27.8%	41 268	60 118	32.8%	43 941	56 159	24.1%
US_m2_s51_t15_c3	42 017	48 055	79.1%	53 697	66 133	59.4%	63 550	70 717	47.8%	47 999	61 312	81.7%	53 318	63 031	61.8%
US_m2_s51_t15_c4	42 017	49 108	74.9%	53 697	63 557	64.0%	63 550	70 082	47.5%	47 181	59 728	85.0%	53 294	66 209	53.3%
US_m2_s51_t20_c3	44 885	51 297	91.8%	66 586	79 192	81.3%	72 027	74 852	66.2%	49 982	62 774	122.8%	58 704	72 683	74.0%
US_m2_s51_t20_c4	44 885	51 529	88.3%	66 586	77 647	85.6%	72 027	76 892	59.9%	49 982	59 767	134.9%	58 704	62 861	100.2%
Avg	**38 637**	**45705**	**50.5%**	**47 945**	**57 871**	**44.4%**	**55 546**	**62 563**	**35.0%**	**43 085**	**56711**	**61.3%**	**46 397**	**56 269**	**42.0%**
US_m3_s51_t5_c3	33 982	39 807	11.5%	34 593	40 772	10.7%	42 065	52 596	7.9%	40 238	53 487	9.5%	35 059	43 600	7.4%
US_m3_s51_t5_c4	32 885	39 376	12.4%	33 490	39 810	13.6%	40 995	52 230	8.5%	38 668	52 492	12.9%	34 002	42 777	10.1%
US_m3_s51_t10_c3	45 491	52 634	53.2%	50 153	55 693	58.7%	61 588	68 004	38.7%	45 861	58 593	73.1%	53 362	62 382	41.6%
US_m3_s51_t10_c4	45 373	53 653	49.7%	51 139	59 271	48.8%	61 125	68 108	36.8%	48 007	63 120	61.3%	52 929	60 199	43.4%
US_m3_s51_t15_c3	48 598	57 064	83.8%	61 569	68 399	89.0%	74 172	80 373	51.6%	49 439	67 085	115.0%	61 687	65 792	85.5%
US_m3_s51_t15_c4	48 598	52 151	101.5%	61 527	69 783	85.3%	74 172	78 889	53.9%	49 439	63 767	124.3%	61 412	64 932	87.4%
US_m3_s51_t20_c3	50 399	51 113	139.2%	74 740	78 438	124.5%	83 566	85 305	70.7%	53 184	57 091	219.6%	65 716	66 531	133.4%
US_m3_s51_t20_c4	50 399	50 782	140.5%	74 740	74 873	136.2%	83 566	85 092	71.3%	53 184	60 760	201.0%	65 716	68 576	127.3%
Avg	**44 466**	**49 572**	**74.0%**	**55 244**	**60 880**	**70.8%**	**65 156**	**71 325**	**42.4%**	**47 252**	**59 549**	**102.1%**	**53735**	**59 349**	**67.0%**

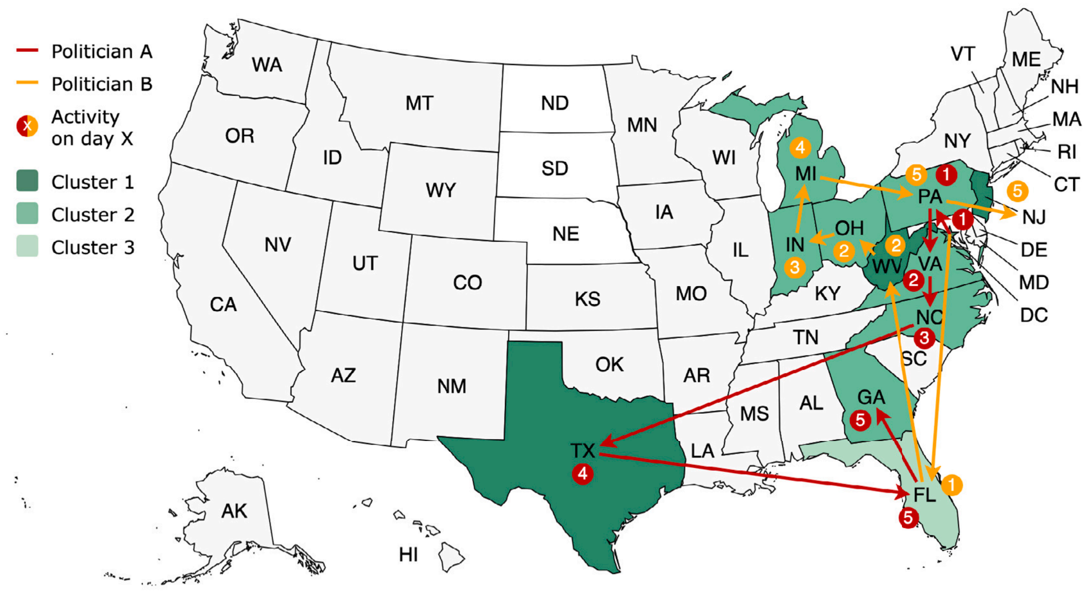

Fig. 5. An optimal solution of instance $US\_m2\_s51\_t5\_c3$ using the convex reward profile ($\Phi^{(cvx)}$).

most challenging, leading to higher optimality gaps. Although functions like the linearly increasing one may appear simpler than the others, they are associated with significantly higher optimality gaps. In addition, for all reward profiles, the optimality gap grows consistently as the size of the time horizon increases. We remark that these considerations are targeted at the behavior of Gurobi when solving the chosen MILP model and must not be referred to the intrinsic complexity of the RM-PRP problem when using different reward profiles.

In Fig. 5 we show a solution of RM-PRP for the instance $US\_m2\_s51\_t5\_c3$ using the reward profile $\Phi^{(cvx)}$. Both politicians hold activities in swing states like Pennsylvania and Florida, as they are highly strategic for delegate accumulation in the election season. Compared to the meetings held during the 2024 US elections, we observe that Pennsylvania also recorded the highest number of activities. Politician A conducts an early campaign event in Pennsylvania, a state with significant delegate influence, indicating a strategic effort to secure key battleground states. Politician B focuses

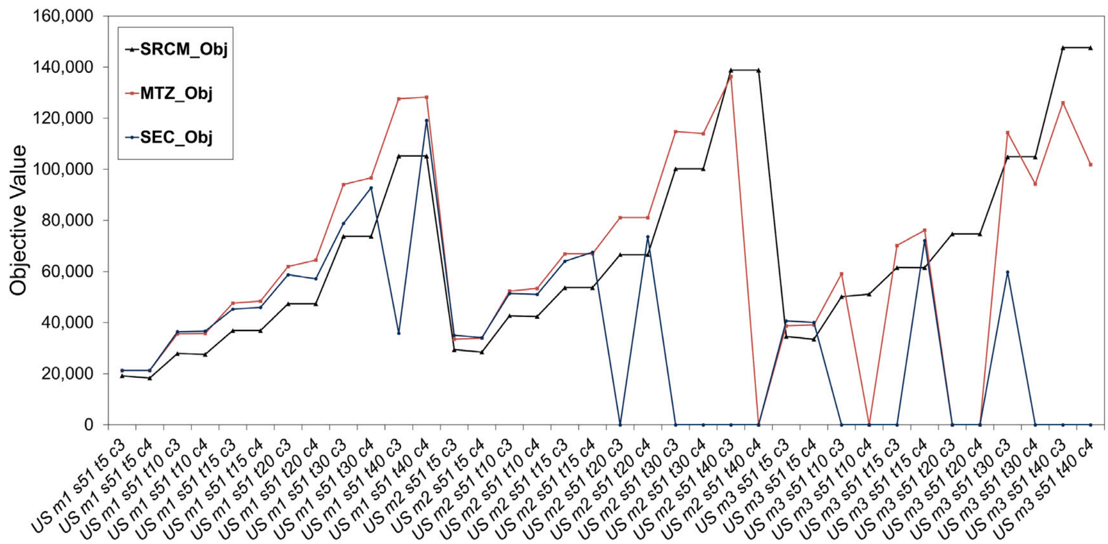

Fig. 6. Performance of SRCM compared to MTZ and SEC models using the convex reward profile ($\Phi^{(\mathrm{cvx})}$).

on Florida, a key state with a large population and strong party base. Elections in most of the states selected by both politicians are usually competitive. As in the 2024 US election, candidates prioritize regional efficiency. For example, Politician *A* clusters events in Pennsylvania, Virginia, and North Carolina to build momentum and rally support from regions with potentially large voter bases. Politician *B*, on the other hand, focuses on the Rust Belt areas (Michigan, Ohio, Indiana), which would strengthen ties with working-class voters, who are crucial in these states. Those election campaign managers whose beliefs align with $\Phi^{(\mathrm{cvx})}$ believe that building momentum through early activities in important states can create a snowball effect [37], where positive media coverage helps attract more votes. Similarly, activities in important states near the end of the campaign strengthen support, reinforce key messages, and boost voter turnout by taking advantage of increased attention in the final stages of the election [38]. Accordingly, both candidates follow the convex reward function's nature, where their schedules prioritize activities in significant states at the beginning and the end of the campaign. Another observation is brief activities in safe states like West Virginia (for politician *B*), which could be more about rallying the base and not swing state persuasion. The activity distribution reflects a strategic focus on states with varying electoral votes, from high (e.g., Pennsylvania, Texas) to lower (e.g., Indiana, West Virginia). Both politicians also cover states from three clusters.

8.4. Performance of SRCM

The RM-PRP is a highly complex combinatorial problem, as shown by large optimality gaps despite connectivity constraints and valid inequalities. Its complexity grows exponentially with the duration of the campaign. In real-world applications, where adjustments to plans and re-optimization may be necessary due to unforeseen events, solving the RM-PRP as a one-off using commercial solvers becomes inefficient. For instance, Trump's 2024 assassination attempt forced rapid campaign redefinition.[9] This highlights the need for a fast algorithm to efficiently solve real-size RM-PRP instances.

In Fig. 6, we report the results for our matheuristic SRCM where we employ the convex reward profile for the experiments. Detailed figures are reported in the second column of Table 3. Each daily model is solved optimally in under 2 s, proving SRCM's efficiency in providing a two-month campaign plan in just 2 min. In 13 of 36 instances, mathematical formulations based on MTZ and SEC constraints failed to find feasible solutions within 3 h, while SRCM found solutions in an average of 38.3 s. For the two instances where optimal solutions are available, SRCM achieves an average objective gap of 11.76%, decreasing to 1.44% for 3-politician instances, showing improved performance as problem size grows. For four instances (*US_m2_s51_t40_c4*, *US_m3_s51_t10_c4*, *US_m3_s51_t20_c3*, and *US_m3_s51_t20_c4*), the commercial solver applied to formulations MTZ and SEC was unable to produce even a feasible solution after 3 h of CPU time, while SRCM was able to find a feasible solution in just 45 s on average. Additionally, for four other instances (*US_m2_s51_t40_c3*, *US_m3_s51_t30_c4*, *US_m3_s51_t40_c3*, and *US_m3_s51_t40_c4*), SRCM not only produced feasible solutions faster but also achieved better solutions within significantly less CPU time compared to formulation MTZ without CC constraints.

Key Observation 4: *SRCM outperforms the exact solver applied to formulations MTZ and SEC in large-scale instances within a 2 min limit. Its lower CPU time allows campaign managers to adaptively update solutions in response to changes in rewards, time constraints, rest days, or budgets.*

8.5. Evaluation of the effectiveness of valid inequalities

Tables 5 and 6 present information about the number and violation of valid inequalities when solving instances with the reward profile $\Phi^{(\mathrm{cvx})}$ and the formulations CC+MTZ and CC+SEC, respectively. Valid inequalities have been dynamically added to both models whenever a violation of at least 0.01 was detected in a fractional solution, reducing the computational overhead compared to loading all of them beforehand. In these tables, the main captions refer to the classes of valid inequalities (the corresponding reference number is reported), Δ indicates the average violation, whereas # indicates the total number of violations that occurred for each family of cuts.

Tables do not include families (63) and (64) as their cardinality is in the order of $\Theta(\overline{m}\cdot\overline{n}^3\cdot\overline{t})$ and separating these inequalities by enumeration would be too expensive.

Key Observation 5: *The SEC-constrained model with CCs outperforms the MTZ-constrained one, showing fewer violations (0.10 vs. 0.15 on average), highlighting its stronger enforcement of feasibility and solution integrity.*

8.6. Sensitivity analysis

In this section, we conduct a sensitivity analysis to understand the impact of varying parameters on the problem solutions. Our analysis

[9] https://www.cbsnews.com/pittsburgh/news/trump-rally-butler-pennsylvania/

Table 5
Cut violations for CC+MTZ model using the convex reward profile ($\Phi^{(cvx)}$).

Instance	(48)		(49)		(50)		(51)		(52)		(53)		(54)		(55)	
	Δ	#	Δ	#	Δ	#	Δ	#	Δ	#	Δ	#	Δ	#	Δ	#
US_m1_s51_t5_c3	0	0	0.098	68	0.106	62	0.049	133	0.081	248	0.081	248	0.049	38	0.194	124
US_m1_s51_t5_c4	0	0	0.118	81	0.131	75	0.051	127	0.079	288	0.079	288	0.047	33	0.183	177
US_m1_s51_t10_c3	0	0	0.105	816	0.127	663	0.043	608	0.079	5652	0.079	5652	0.040	142	0.154	1219
US_m1_s51_t10_c4	0	0	0.091	636	0.118	486	0.043	579	0.073	5324	0.073	5324	0.041	126	0.156	1263
US_m1_s51_t15_c3	0	0	0.082	216	0.097	141	0.039	651	0.062	6506	0.062	6506	0.045	149	0.161	497
US_m1_s51_t15_c4	0	0	0.106	321	0.129	226	0.041	687	0.063	7217	0.063	7217	0.043	151	0.161	576
US_m1_s51_t20_c3	0	0	0.143	61	0.170	47	0.042	782	0.063	5767	0.063	5767	0.039	179	0.152	121
US_m1_s51_t20_c4	0	0	0.106	35	0.125	25	0.043	770	0.062	5544	0.062	5544	0.042	173	0.149	80
US_m1_s51_t30_c3	0	0	0.039	4	0.017	1	0.033	681	0.054	2525	0.054	2525	0.036	141	0.119	14
US_m1_s51_t30_c4	0	0	0.047	5	0.056	4	0.033	709	0.059	3220	0.059	3220	0.035	155	0.143	12
US_m1_s51_t40_c3	0	0	0.107	1	0.107	1	0.033	945	0.049	1461	0.049	1461	0.034	204	0.166	2
US_m1_s51_t40_c4	0	0	0.118	1	0.118	1	0.033	885	0.048	1533	0.048	1533	0.036	173	0.092	4
US_m2_s51_t5_c3	0	0	0.093	2454	0.108	2064	0.044	422	0.076	7054	0.076	7054	0.038	112	0.191	3862
US_m2_s51_t5_c4	0	0	0.101	1634	0.113	1381	0.045	612	0.071	6291	0.071	6291	0.040	144	0.175	3216
US_m2_s51_t10_c3	0	0	0.127	76	0.155	57	0.041	854	0.060	4959	0.060	4959	0.041	191	0.162	153
US_m2_s51_t10_c4	0	0	0.112	68	0.144	46	0.040	876	0.060	5136	0.060	5136	0.039	212	0.153	144
US_m2_s51_t15_c3	0	0	0.083	9	0.145	8	0.033	622	0.052	2072	0.052	2072	0.037	117	0.128	12
US_m2_s51_t15_c4	0	0	0.040	8	0.056	4	0.035	634	0.056	2668	0.056	2668	0.039	115	0.113	14
US_m2_s51_t20_c3	0	0	0.099	2	0.099	2	0.037	723	0.048	1264	0.048	1264	0.037	162	0.111	5
US_m2_s51_t20_c4	0	0	0.102	2	0.102	2	0.036	766	0.049	1460	0.049	1460	0.034	169	0.120	9
US_m2_s51_t30_c3	0	0	0.074	2	0.074	2	0.038	1035	0.050	1796	0.050	1796	0.037	267	0.149	5
US_m2_s51_t30_c4	0	0	0.049	1	0.049	1	0.038	1019	0.049	1819	0.049	1819	0.039	264	0.098	6
US_m2_s51_t40_c3	0	0	0.038	2	0.038	2	0.039	1270	0.050	1962	0.050	1962	0.036	352	0.135	2
US_m2_s51_t40_c4	0	0	0.041	1	0.041	1	0.038	1312	0.051	1932	0.051	1932	0.036	338	0.071	3
US_m3_s51_t5_c3	0	0	0.110	514	0.127	402	0.042	679	0.068	5729	0.068	5729	0.044	160	0.174	2094
US_m3_s51_t5_c4	0	0	0.099	412	0.119	318	0.043	692	0.066	4908	0.066	4908	0.044	166	0.175	2009
US_m3_s51_t10_c3	0	0	0.106	18	0.143	11	0.033	772	0.057	3847	0.057	3847	0.031	174	0.217	27
US_m3_s51_t10_c4	0	0	0.103	17	0.135	11	0.033	703	0.055	3582	0.055	3582	0.032	157	0.172	30
US_m3_s51_t15_c3	0	0	0.060	12	0.072	6	0.035	844	0.047	1968	0.047	1968	0.034	211	0.178	7
US_m3_s51_t15_c4	0	0	0.072	9	0.058	4	0.034	825	0.048	1659	0.048	1659	0.034	202	0.195	6
US_m3_s51_t20_c3	0	0	0.087	9	0.072	3	0.036	993	0.047	1817	0.047	1817	0.036	245	0.146	6
US_m3_s51_t20_c4	0	0	0.072	3	0.072	3	0.036	1043	0.045	1886	0.045	1886	0.036	247	0.184	8
US_m3_s51_t30_c3	0	0	0.050	5	0.070	3	0.036	1355	0.050	2186	0.050	2186	0.036	331	0.199	3
US_m3_s51_t30_c4	0	0	0.054	8	0.052	5	0.037	1337	0.049	2291	0.049	2291	0.037	322	0.166	2
US_m3_s51_t40_c3	0	0	0.036	2	0.036	2	0.048	1007	0.070	888	0.070	888	0.037	338	0.092	1
US_m3_s51_t40_c4	0	0	0.036	2	0.036	2	0.048	968	0.075	902	0.075	902	0.037	330	0	0

Instance	(56)		(57)		(58)		(59)		(60)		(61)		(62)	
	Δ	#	Δ	#	Δ	#	Δ	#	Δ	#	Δ	#	Δ	#
US_m1_s51_t5_c3	0.296	12	0.264	12	0	0	0	0	0	0	0	0	0	0
US_m1_s51_t5_c4	0.255	18	0.150	14	0	0	0	0	0	0	0	0	0	0
US_m1_s51_t10_c3	0.203	527	0.156	306	0	0	0.312	515	0.101	7	0.101	7	0	0
US_m1_s51_t10_c4	0.226	450	0.165	355	0	0	0.333	516	0.107	29	0.107	29	0	0
US_m1_s51_t15_c3	0.233	452	0.224	168	0.037	33	0.355	793	0.129	874	0.129	874	0	0
US_m1_s51_t15_c4	0.205	554	0.170	210	0.036	79	0.357	712	0.109	653	0.109	653	0	0
US_m1_s51_t20_c3	0.296	273	0.364	39	0.040	60	0.449	928	0.180	3872	0.178	3903	0.153	35
US_m1_s51_t20_c4	0.289	196	0.085	14	0.047	64	0.502	810	0.176	3716	0.175	3728	0.212	26
US_m1_s51_t30_c3	0.336	560	0	0	0.038	6	0.713	464	0.506	2694	0.473	2849	0.289	6
US_m1_s51_t30_c4	0.365	518	0	0	0.032	11	0.684	538	0.465	2910	0.429	3170	0.480	7
US_m1_s51_t40_c3	0.361	796	0	0	0.033	5	0.720	281	0.664	1502	0.419	2451	0.300	1
US_m1_s51_t40_c4	0.338	1036	0	0	0.033	2	0.778	340	0.703	1361	0.478	2019	0	0
US_m2_s51_t5_c3	0.169	701	0.235	461	0	0	0.140	42	0.100	6	0.100	6	0.091	1
US_m2_s51_t5_c4	0.139	592	0.257	292	0	0	0.124	29	0.058	3	0.058	3	0.059	1
US_m2_s51_t10_c3	0.245	506	0.198	77	0.039	25	0.315	681	0.272	446	0.223	569	0.182	78
US_m2_s51_t10_c4	0.245	661	0.284	53	0.072	21	0.305	705	0.197	528	0.155	715	0.191	161
US_m2_s51_t15_c3	0.225	151	0	0	0.030	2	0.557	408	0.265	356	0.146	797	0.304	45
US_m2_s51_t15_c4	0.239	187	0	0	0.023	3	0.464	505	0.208	248	0.117	638	0.338	53
US_m2_s51_t20_c3	0.337	82	0	0	0	0	0.476	191	0.142	149	0.134	222	0.309	37
US_m2_s51_t20_c4	0.327	99	0	0	0	0	0.452	246	0.096	82	0.101	154	0.289	39
US_m2_s51_t30_c3	0.304	1268	0	0	0	0	0.620	338	0.319	378	0.188	809	0.250	32
US_m2_s51_t30_c4	0.314	1420	0	0	0	0	0.656	327	0.281	362	0.203	623	0.247	35
US_m2_s51_t40_c3	0.287	2221	0	0	0	0	0.598	366	0.471	387	0.248	1003	0.251	30
US_m2_s51_t40_c4	0.321	2114	0	0	0	0	0.618	364	0.472	351	0.224	1029	0.251	30
US_m3_s51_t5_c3	0.153	685	0.181	167	0	0	0.064	73	0.095	45	0.095	45	0.096	26
US_m3_s51_t5_c4	0.174	645	0.269	124	0	0	0.072	69	0.069	14	0.095	14	0.108	54
US_m3_s51_t10_c3	0.265	278	0.132	6	0.152	9	0.364	381	0.248	215	0.130	593	0.272	82
US_m3_s51_t10_c4	0.239	251	0.683	17	0.087	8	0.441	493	0.396	66	0.216	238	0.378	94
US_m3_s51_t15_c3	0.277	139	0	0	0.048	4	0.610	256	1.625	23	0.933	43	0.302	59
US_m3_s51_t15_c4	0.276	121	0	0	0.051	1	0.552	225	1.864	11	0.694	36	0.313	75
US_m3_s51_t20_c3	0.287	131	0	0	0	0	0.550	239	2.662	16	1.560	24	0.264	64
US_m3_s51_t20_c4	0.281	135	0	0	0	0	0.525	256	0.754	16	0.540	19	0.284	43
US_m3_s51_t30_c3	0.298	204	0	0	0	0	0.615	314	0	0	0.125	17	0.186	103
US_m3_s51_t30_c4	0.278	198	0.046	4	0	0	0.618	272	0	0	0.137	13	0.188	110
US_m3_s51_t40_c3	0.438	130	0	0	0	0	0.449	63	0	0	0.262	19	0.195	158
US_m3_s51_t40_c4	0.428	133	0	0	0	0	0.484	62	0	0	0.266	18	0.187	162

Table 6
Cut violations for CC+SEC model using the convex reward profile ($\Phi^{(cvx)}$).

Instance	(48)		(49)		(50)		(51)		(52)		(53)		(54)		(55)	
	Δ	#	Δ	#	Δ	#	Δ	#	Δ	#	Δ	#	Δ	#	Δ	#
US_m1_s51_t5_c3	0	0	0.217	28	0.230	26	0.056	109	0.080	127	0.080	127	0.046	22	0.166	80
US_m1_s51_t5_c4	0	0	0.173	18	0.195	15	0.050	109	0.081	121	0.081	121	0.051	23	0.174	70
US_m1_s51_t10_c3	0	0	0.153	50	0.169	43	0.039	280	0.070	315	0.070	315	0.039	58	0.156	159
US_m1_s51_t10_c4	0	0	0.145	41	0.157	36	0.037	270	0.068	333	0.068	333	0.038	50	0.174	141
US_m1_s51_t15_c3	0	0	0.166	35	0.164	33	0.038	426	0.061	480	0.061	480	0.043	82	0.130	211
US_m1_s51_t15_c4	0	0	0.117	33	0.128	27	0.043	439	0.061	509	0.061	509	0.042	100	0.125	222
US_m1_s51_t20_c3	0	0	0.159	33	0.166	30	0.038	568	0.052	610	0.052	610	0.041	129	0.187	178
US_m1_s51_t20_c4	0	0	0.148	39	0.167	36	0.037	566	0.059	646	0.059	646	0.040	107	0.146	185
US_m1_s51_t30_c3	0	0	0.256	5	0.260	5	0.033	700	0.048	726	0.048	726	0.038	162	0.177	5
US_m1_s51_t30_c4	0	0	0.035	2	0.033	2	0.033	716	0.049	734	0.049	734	0.036	150	0.176	8
US_m1_s51_t40_c3	0	0	0.090	1	0.090	1	0.036	1059	0.050	1095	0.050	1095	0.036	193	0.131	4
US_m1_s51_t40_c4	0	0	0.061	2	0.061	2	0.038	905	0.056	928	0.056	928	0.037	181	0.180	4
US_m2_s51_t5_c3	0	0	0.170	79	0.188	64	0.046	289	0.065	354	0.065	354	0.040	75	0.181	204
US_m2_s51_t5_c4	0	0	0.127	90	0.135	70	0.042	318	0.062	357	0.062	357	0.040	69	0.178	301
US_m2_s51_t10_c3	0	0	0.184	43	0.217	35	0.041	616	0.051	726	0.051	726	0.040	149	0.145	218
US_m2_s51_t10_c4	0	0	0.173	44	0.187	38	0.038	607	0.053	737	0.053	737	0.038	128	0.138	206
US_m2_s51_t15_c3	0	0	0.061	6	0.061	6	0.033	758	0.051	804	0.051	804	0.037	142	0.136	41
US_m2_s51_t15_c4	0	0	0.061	3	0.061	3	0.034	795	0.050	857	0.050	857	0.036	151	0.201	36
US_m2_s51_t20_c3	0	0	0.106	4	0.137	3	0.034	884	0.052	926	0.052	926	0.036	203	0.140	6
US_m2_s51_t20_c4	0	0	0.094	4	0.094	4	0.035	861	0.052	909	0.052	909	0.036	214	0.112	5
US_m2_s51_t30_c3	0	0	0	0	0	0	0.040	1461	0.056	1532	0.056	1532	0.039	389	0.112	5
US_m2_s51_t30_c4	0	0	0.090	3	0.090	3	0.040	1560	0.054	1761	0.054	1761	0.039	417	0.050	5
US_m2_s51_t40_c3	0	0	0	0	0	0	0.039	2255	0.060	2767	0.060	2767	0.036	592	0.091	3
US_m2_s51_t40_c4	0	0	0	0	0	0	0.038	2298	0.060	2892	0.060	2892	0.036	570	0	0
US_m3_s51_t5_c3	0	0	0.196	57	0.211	47	0.039	468	0.057	552	0.057	552	0.040	110	0.146	308
US_m3_s51_t5_c4	0	0	0.126	74	0.149	57	0.038	483	0.058	556	0.058	556	0.040	108	0.163	376
US_m3_s51_t10_c3	0	0	0.196	19	0.210	16	0.034	896	0.045	1047	0.045	1047	0.032	182	0.144	109
US_m3_s51_t10_c4	0	0	0.110	13	0.135	10	0.034	872	0.047	1011	0.047	1011	0.033	191	0.166	83
US_m3_s51_t15_c3	0	0	0.092	6	0.098	2	0.038	964	0.054	1035	0.054	1035	0.037	245	0.135	8
US_m3_s51_t15_c4	0	0	0.075	10	0.078	4	0.035	864	0.051	1051	0.051	1051	0.036	232	0.140	8
US_m3_s51_t20_c3	0	0	0.119	9	0.128	3	0.039	1327	0.060	1329	0.060	1329	0.035	358	0.226	7
US_m3_s51_t20_c4	0	0	0.115	7	0.122	1	0.040	1362	0.062	1592	0.062	1592	0.036	399	0.108	4
US_m3_s51_t30_c3	0	0	0.128	20	0.081	13	0.037	2591	0.065	3648	0.065	3648	0.035	679	0.148	8
US_m3_s51_t30_c4	0	0	0.064	14	0.096	3	0.037	2666	0.069	3617	0.069	3617	0.037	723	0.134	5
US_m3_s51_t40_c3	0	0	0	0	0	0	0.037	4504	0.074	7607	0.074	7607	0.035	1320	0.100	9
US_m3_s51_t40_c4	0	0	0	0	0	0	0.038	3631	0.066	5467	0.066	5467	0.034	983	0.090	4

Instance	(56)		(57)		(58)		(59)		(60)		(61)		(62)	
	Δ	#	Δ	#	Δ	#	Δ	#	Δ	#	Δ	#	Δ	#
US_m1_s51_t5_c3	0.478	5	0.454	5	0	0	0	0	0	0	0	0	0	0
US_m1_s51_t5_c4	0.560	4	0.231	5	0	0	0	0	0	0	0	0	0	0
US_m1_s51_t10_c3	0.459	10	0.153	611	0	0	0.238	10	0.078	4	0.078	4	0	0
US_m1_s51_t10_c4	0.451	10	0.206	606	0	0	0.381	10	0.090	4	0.090	4	0	0
US_m1_s51_t15_c3	0.495	15	0.232	463	0.047	45	0.444	15	0.082	84	0.082	84	0	0
US_m1_s51_t15_c4	0.493	15	0.186	365	0.033	47	0.369	15	0.070	82	0.070	82	0	0
US_m1_s51_t20_c3	0.423	20	0.265	251	0.045	87	0.499	20	0.104	195	0.084	267	0.238	29
US_m1_s51_t20_c4	0.442	20	0.243	270	0.038	61	0.468	20	0.125	174	0.102	237	0.249	27
US_m1_s51_t30_c3	0.511	29	0.360	12	0.029	13	0.631	30	0.293	378	0.112	1335	0.422	6
US_m1_s51_t30_c4	0.511	29	0	0	0.030	18	0.661	30	0.366	379	0.189	851	0.369	23
US_m1_s51_t40_c3	0.441	77	0	0	0	0	0.714	55	0.677	916	0.404	1658	0	0
US_m1_s51_t40_c4	0.453	76	0	0	0.030	5	0.627	53	0.736	793	0.486	1268	0.208	2
US_m2_s51_t5_c3	0.416	10	0.314	742	0	0	0.092	3	0.122	4	0.122	4	0	0
US_m2_s51_t5_c4	0.390	10	0.259	858	0	0	0.130	3	0.052	4	0.052	4	0.066	3
US_m2_s51_t10_c3	0.445	20	0.289	332	0.051	30	0.326	20	0.142	98	0.096	222	0.170	118
US_m2_s51_t10_c4	0.464	20	0.254	413	0.069	34	0.325	20	0.206	93	0.109	216	0.168	110
US_m2_s51_t15_c3	0.524	28	0.134	26	0.037	21	0.507	30	0.383	178	0.123	984	0.311	92
US_m2_s51_t15_c4	0.510	29	0.185	32	0.030	8	0.524	30	0.330	192	0.103	1137	0.359	104
US_m2_s51_t20_c3	0.451	38	0	0	0.042	2	0.469	40	0.569	290	0.215	893	0.257	24
US_m2_s51_t20_c4	0.459	38	0	0	0.019	5	0.442	40	0.565	264	0.174	1076	0.258	28
US_m2_s51_t30_c3	0.381	108	0	0	0	0	0.594	92	0.236	177	0.174	376	0.250	25
US_m2_s51_t30_c4	0.380	109	0	0	0	0	0.549	102	0.250	239	0.181	458	0.247	41
US_m2_s51_t40_c3	0.369	151	0	0	0	0	0.573	144	0.668	436	0.516	637	0.234	33
US_m2_s51_t40_c4	0.364	154	0	0	0	0	0.613	186	0.667	489	0.531	700	0.251	30
US_m3_s51_t5_c3	0.451	15	0.233	451	0	0	0.121	7	0.124	7	0.095	10	0.063	19
US_m3_s51_t5_c4	0.472	15	0.252	479	0	0	0.113	6	0.150	7	0.125	10	0.059	15
US_m3_s51_t10_c3	0.451	29	0.273	106	0.097	23	0.388	30	0.367	103	0.138	545	0.265	173
US_m3_s51_t10_c4	0.472	28	0.386	117	0.056	18	0.383	30	0.249	105	0.092	698	0.227	167
US_m3_s51_t15_c3	0.411	74	0.035	2	0.076	1	0.483	50	1.719	43	0.864	99	0.330	45
US_m3_s51_t15_c4	0.487	42	0	0	0.156	5	0.508	43	0.992	85	0.542	200	0.370	98
US_m3_s51_t20_c3	0.409	96	0	0	0	0	0.530	71	0.115	7	0.189	39	0.334	49
US_m3_s51_t20_c4	0.381	101	0	0	0	0	0.542	80	2.860	16	1.909	25	0.223	74
US_m3_s51_t30_c3	0.375	154	0	0	0	0	0.593	183	0	0	0.134	70	0.146	180
US_m3_s51_t30_c4	0.361	158	0.013	1	0	0	0.525	176	0	0	0.096	47	0.164	277
US_m3_s51_t40_c3	0.354	199	0	0	0	0	0.481	328	0	0	0.139	67	0.165	557
US_m3_s51_t40_c4	0.355	207	0	0	0	0	0.564	261	0	0	0.156	57	0.156	333

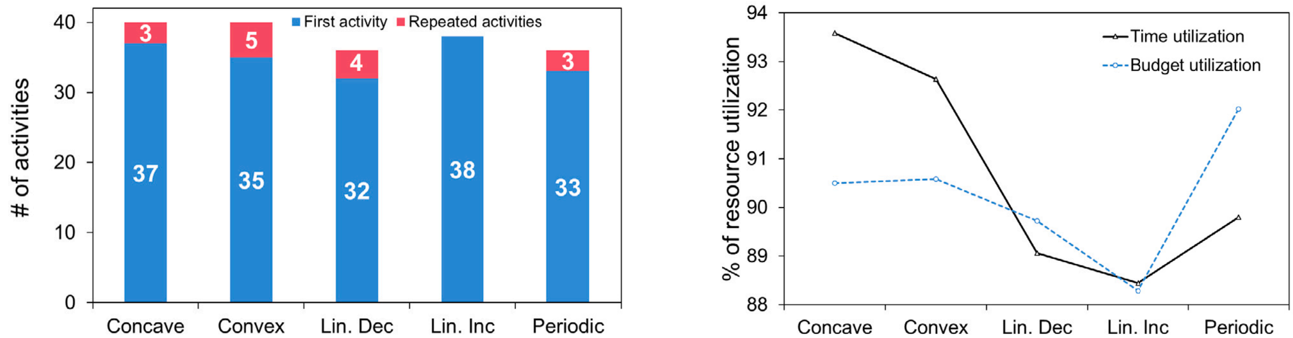

(a) Number of activities for different reward profiles.

(b) Resource utilization for different reward profiles.

Fig. 7. Sensitivity analysis on instances with optimal solutions for different reward profiles.

varies reward functions (Section 8.6.1), budgets (Section 8.6.2), and rest days (Section 8.6.3).

8.6.1. Impact of the reward profile function on number of activities and resource utilization

We conducted a sensitivity analysis by modifying the reward profile Φ on all instances. Tables 7–9 contain the following campaign metrics for each politician: the total number of activities separating first activities (*# First activities*) from subsequent ones (*# Subsequent activities*), the ratio between the total activity time over the maximum duration of a daily tour q (*Activity time (%)*), the ratio between the total travel time over q (*Traveling time (%)*), and the ratio between the consumed budget over the available one (*Budget consumption (%)*).

Fig. 7 shows variations in activities and resource for the different reward profiles on the four instances where we find an optimal solution (*US_m1_s51_t5_c3*, *US_m1_s51_t5_c4*, *US_m1_s51_t10_c3*, and *US_m2_s51_t5_c3*).

Fig. 7(a) plots the number of first and repeated activities conducted by politicians, with the figures representing the sums across all four selected instances. The results indicate functions $\Phi^{(\mathrm{cvx})}$ and $\Phi^{(\mathrm{ccv})}$ yield the highest total number of activities (40 each), while $\Phi^{(\mathrm{dec})}$ results in the fewest, totaling 36. This suggests that campaign managers using $\Phi^{(\mathrm{cvx})}$ or $\Phi^{(\mathrm{ccv})}$ reward profiles are likely to conduct more activities, whereas decision makers using $\Phi^{(\mathrm{dec})}$ should not expect to conduct as many activities as those using the other two functions. In terms of repeated activities, $\Phi^{(\mathrm{cvx})}$ results in five repeated activities, which makes it more suitable for campaign managers who believe that repeated activities will not lead to voter fatigue. In contrast, the $\Phi^{(\mathrm{inc})}$ function results in zero repeated activities, likely due to its tendency to prioritize high-reward cities early in the campaign.

Fig. 7(b) displays the average percentage of resource utilization for all politicians, where resource utilization is calculated as the ratio of used resources to allocated resources. We observe that while the $\Phi^{(\mathrm{ccv})}$ function achieves the highest time utilization, the $\Phi^{(\mathrm{per})}$ function leads to the highest budget utilization. On the other hand, the $\Phi^{(\mathrm{inc})}$ profile consistently exhibits the lowest time and budget utilization among all reward functions. Comparing this with the number of repeated activities, where $\Phi^{(\mathrm{inc})}$ function results in zero repeated activities, we infer that decision makers prioritizing holding activities in as many locations as possible should expect lower resource utilization.

8.6.2. Impact of varying budget

In RM-PRP, the budget is predetermined, making its sensitivity analysis highly relevant for practical applications. For this experiment, we use instance *US_m2_s51_t5_c3* under the reward profile $\Phi^{(\mathrm{cvx})}$ with the optimal objective value of 35010 and vary the value of b_m from 70% to 130%, with a step size of 10%. We plot the summary of results in Fig. 8(a) and present the detailed values in Table 10 whose columns have the same meaning as those in Table 7. The results indicate that increasing the budget from 70% to 80% and from 80% to 90% improves the objective function by 14% and 12%, respectively. However, the improvement between 90% to 110% is marginal, with only 3% and 2% increases. Increasing the budget from 110% to 120% and from 120% to 130% yields no improvement and is ineffective, likely due to other constraints imposed by the problem. A similar pattern is observed in the percentage of the budget spent, for the same reason. The results also highlight that reducing the budget impacts the percentage of time allocated to hold activities more significantly than the percentage of time spent on traveling.

8.6.3. Impact of varying rest days

In addition to the reward profile function and budget, the number of rest days included in the weekly itinerary of politicians also affects the solutions. In election logistics, this influences the number of locations chosen to hold one or more activities, and thus the overall effectiveness of the campaign. We analyze the influence of this parameter using instance *US_m1_s51_t10_c4* with $\Phi^{(\mathrm{cvx})}$ by changing parameter e from 0 to 4 with a step size of 1. The results are shown in Fig. 8(b) along with detailed figures presented in Table 11. We observe that, intuitively, the objective value deteriorates significantly as the number of rest days increases from 0 to 4, with decreases of −1.4%, −5.1%, −6.3%, and −12.7%, respectively. This suggests a clear negative relationship between the number of rest days and the overall performance of the campaign. In terms of the number of first activities, no notable difference is observed when e is set to 1, 2, or 3. However, once e exceeds 3, key performance indicators deteriorate sharply, which indicates a threshold beyond which the effectiveness of the campaign significantly declines. For election campaign managers with similar reward mechanisms, this value could serve as a critical cutoff point to ensure an effective solution. Given that the budget remains fixed while varying the parameter e, the results also underscore the impact of increasing rest days on resource utilization. Specifically, as the number of rest days increases, budget resource utilization declines significantly, suggesting that allocating more time for rest periods detracts from the overall efficiency of resource expenditure.

9. Conclusion

In this paper, we introduce and investigate the Reward-driven Multi-period Clustered Routing Problem (RM-PRP), a new optimization problem inspired by the complexities of US presidential election campaigns. RM-PRP optimizes the routing and scheduling of multiple politicians from the same political party while accounting for real constraints on budget and rest days as well as the partition of cities into clusters according to their relevance and the possibility to embed different reward profiles. This problem is both practically and theoretically significant due to its computational complexity and its potential to optimize election logistics, while also extending classical routing models in the

Table 7
Solution analysis for concave and convex reward profiles ($\Phi^{(ccv)}$ and $\Phi^{(cvx)}$).

$\Phi^{(ccv)}$

Instance	Obj	# First activities			# Subsequent activities			Activity time (%)			Traveling time (%)			Budget consumption (%)		
		Repr 1			Repr 1			Repr 1			Repr 1			Repr 1		
US_m1_s51_t5_c3	20 896	7			0			48.0%			47.5%			88.4%		
US_m1_s51_t5_c4	20 896	7			0			48.0%			47.5%			88.4%		
US_m1_s51_t10_c3	32 814	10			2			42.0%			44.1%			81.0%		
US_m1_s51_t10_c4	32 982	9			3			42.0%			44.3%			84.6%		
US_m1_s51_t15_c3	38 942	14			3			39.0%			43.0%			76.6%		
US_m1_s51_t15_c4	38 466	14			3			39.3%			40.8%			78.0%		
US_m1_s51_t20_c3	40 423	17			5			37.5%			43.7%			73.0%		
US_m1_s51_t20_c4	39 305	18			4			37.2%			44.8%			73.2%		
		Repr 1	Repr 2		Repr 1	Repr 2		Repr 1	Repr 2		Repr 1	Repr 2		Repr 1	Repr 2	
US_m2_s51_t5_c3	34 226	7	6		0	1		49.0%	47.0%		48.0%	46.8%		94.8%	99.9%	
US_m2_s51_t5_c4	33 908	7	5		0	2		49.0%	48.0%		48.0%	40.6%		94.8%	99.7%	
US_m2_s51_t10_c3	48 115	9	9		3	2		42.0%	36.5%		47.8%	47.2%		85.5%	88.0%	
US_m2_s51_t10_c4	49 399	9	9		3	3		41.5%	40.5%		45.3%	48.0%		85.2%	90.4%	
US_m2_s51_t15_c3	48 055	8	12		5	3		30.0%	33.3%		47.0%	37.8%		74.3%	73.2%	
US_m2_s51_t15_c4	49 108	10	11		6	3		36.0%	31.3%		42.1%	46.4%		71.9%	79.7%	
US_m2_s51_t20_c3	51 297	13	13		8	8		34.0%	35.2%		46.8%	46.0%		66.6%	82.5%	
US_m2_s51_t20_c4	51 529	15	11		4	10		31.8%	35.5%		45.9%	40.9%		64.1%	82.1%	
		Repr 1	Repr 2	Repr 3	Repr 1	Repr 2	Repr 3	Repr 1	Repr 2	Repr 3	Repr 1	Repr 2	Repr 3	Repr 1	Repr 2	Repr 3
US_m3_s51_t5_c3	39 807	6	5	4	0	1	1	42.0%	42.0%	33.0%	48.4%	43.5%	39.8%	91.8%	97.1%	97.3%
US_m3_s51_t5_c4	39 376	6	5	6	0	2	0	42.0%	48.0%	38.0%	44.2%	39.6%	36.1%	89.9%	99.7%	97.2%
US_m3_s51_t10_c3	52 634	8	8	6	3	3	4	37.0%	38.0%	33.5%	49.0%	46.5%	38.4%	76.7%	94.3%	95.1%
US_m3_s51_t10_c4	53 653	9	7	6	2	4	3	37.0%	37.5%	30.0%	45.4%	48.9%	45.9%	72.2%	93.2%	99.6%
US_m3_s51_t15_c3	57 064	9	10	10	7	5	5	36.3%	33.3%	32.3%	45.3%	43.2%	49.0%	74.5%	81.9%	97.5%
US_m3_s51_t15_c4	52 151	9	10	6	5	3	5	31.7%	28.7%	24.7%	52.1%	42.4%	35.3%	69.9%	76.1%	85.6%
US_m3_s51_t20_c3	51 113	9	11	7	8	5	7	28.5%	27.3%	23.2%	34.9%	45.6%	40.5%	58.2%	77.7%	80.5%
US_m3_s51_t20_c4	50 782	10	10	6	7	5	7	28.5%	25.5%	21.8%	36.0%	36.7%	35.9%	58.1%	73.5%	74.4%

$\Phi^{(cvx)}$

Instance	Obj	# First activities			# Subsequent activities			Activity time (%)			Traveling time (%)			Budget consumption (%)		
		Repr 1			Repr 1			Repr 1			Repr 1			Repr 1		
US_m1_s51_t5_c3	21 260	7			0			48.0%			47.7%			90.4%		
US_m1_s51_t5_c4	21 260	7			0			48.0%			47.7%			90.4%		
US_m1_s51_t10_c3	36 340	9			3			41.5%			45.6%			83.6%		
US_m1_s51_t10_c4	36 640	9			2			38.5%			43.8%			79.7%		
US_m1_s51_t15_c3	49 086	14			3			39.0%			44.7%			75.9%		
US_m1_s51_t15_c4	49 111	14			3			39.0%			43.6%			75.4%		
US_m1_s51_t20_c3	62 173	18			4			37.2%			46.0%			73.6%		
US_m1_s51_t20_c4	61 990	16			5			35.5%			44.3%			70.5%		
		Repr 1	Repr 2		Repr 1	Repr 2		Repr 1	Repr 2		Repr 1	Repr 2		Repr 1	Repr 2	
US_m2_s51_t5_c3	35 010	6	6		1	1		49.0%	48.0%		42.8%	44.9%		89.3%	99.2%	
US_m2_s51_t5_c4	34 514	7	5		0	2		49.0%	47.0%		48.0%	43.7%		94.8%	99.9%	
US_m2_s51_t10_c3	54 065	10	7		2	4		42.0%	37.0%		41.5%	50.0%		79.6%	93.9%	
US_m2_s51_t10_c4	52 848	8	10		3	2		38.0%	40.5%		42.1%	48.0%		70.5%	99.9%	
US_m2_s51_t15_c3	66 133	11	11		4	5		34.0%	35.3%		49.2%	40.3%		71.7%	81.5%	
US_m2_s51_t15_c4	63 557	11	12		4	3		34.0%	33.0%		45.0%	42.0%		69.7%	75.2%	
US_m2_s51_t20_c3	79 192	11	13		8	7		31.8%	33.5%		39.7%	42.2%		63.4%	78.0%	
US_m2_s51_t20_c4	77 647	13	13		5	7		29.5%	34.0%		44.7%	40.3%		61.6%	78.1%	
		Repr 1	Repr 2	Repr 3	Repr 1	Repr 2	Repr 3	Repr 1	Repr 2	Repr 3	Repr 1	Repr 2	Repr 3	Repr 1	Repr 2	Repr 3
US_m3_s51_t5_c3	40 772	6	5	4	0	2	1	42.0%	47.0%	34.0%	50.5%	41.9%	44.0%	93.1%	99.8%	98.3%
US_m3_s51_t5_c4	39 810	6	5	6	1	1	0	49.0%	41.0%	38.0%	35.2%	45.3%	39.7%	83.3%	98.9%	98.9%
US_m3_s51_t10_c3	55 693	9	7	5	1	4	4	33.0%	37.0%	31.0%	46.7%	43.1%	44.6%	70.1%	86.7%	99.8%
US_m3_s51_t10_c4	59 271	7	10	6	3	2	4	34.5%	40.5%	32.5%	46.9%	43.8%	42.5%	66.8%	92.8%	98.9%
US_m3_s51_t15_c3	68 399	11	9	10	2	6	4	29.0%	33.0%	31.0%	43.9%	43.4%	40.9%	63.0%	79.3%	92.7%
US_m3_s51_t15_c4	69 783	11	8	10	3	7	4	30.7%	34.3%	31.0%	42.1%	48.1%	44.9%	64.4%	86.2%	96.1%
US_m3_s51_t20_c3	78 438	10	9	8	5	9	6	25.0%	30.8%	23.0%	40.8%	39.0%	37.5%	56.9%	76.5%	80.6%
US_m3_s51_t20_c4	74 873	10	7	8	5	8	6	25.0%	25.8%	23.2%	39.0%	34.0%	32.1%	56.3%	69.1%	73.2%

literature. To address this problem, we develop multiple formulations and introduce new valid inequalities to tighten the model and generalize connectivity and subtour elimination constraints. We also propose five distinct reward trends, each reflecting different decision-making perspectives in election logistics. We introduce 36 new benchmark instances for the problem tailored to US presidential elections involving up to 3 politicians, 51 states, 40 days, and 4 clusters. We thoroughly evaluate and compare the reward trends to provide insights into their complexities. Furthermore, we design an efficient matheuristic, the Sequential Route Construction Matheuristic, which outperforms commercial MILP solvers in generating feasible solutions quickly for large instances where solvers fail to produce a solution. We also conduct a sensitivity analysis to examine how variations in problem parameters influence key performance indicators. Our solutions indicate that

Table 8
Solution analysis for linearly decreasing and linearly increasing reward profiles ($\Phi^{(\mathrm{dec})}$ and $\Phi^{(\mathrm{inc})}$).

$\Phi^{(\mathrm{dec})}$

Instance	Obj	# First activities			# Subsequent activities			Activity time (%)			Traveling time (%)			Budget consumption (%)		
		Repr 1			Repr 1			Repr 1			Repr 1			Repr 1		
US_m1_s51_t5_c3	27 952	6			0			42.0%			50.6%			94.1%		
US_m1_s51_t5_c4	27 952	6			0			42.0%			50.6%			94.1%		
US_m1_s51_t10_c3	40 242	9			2			38.5%			45.1%			80.9%		
US_m1_s51_t10_c4	40 242	9			2			38.5%			45.2%			80.9%		
US_m1_s51_t15_c3	49 653	13			4			39.0%			44.1%			75.9%		
US_m1_s51_t15_c4	50 247	11			5			37.0%			45.3%			74.4%		
US_m1_s51_t20_c3	58 503	14			6			34.5%			46.9%			73.7%		
US_m1_s51_t20_c4	56 635	16			6			37.5%			44.4%			72.5%		
		Repr 1	Repr 2		Repr 1	Repr 2		Repr 1	Repr 2		Repr 1	Repr 2		Repr 1	Repr 2	
US_m2_s51_t5_c3	44 191	6	5		1	1		48.0%	41.0%		44.2%	43.3%		80.9%	98.6%	
US_m2_s51_t5_c4	44 191	6	5		1	1		48.0%	41.0%		44.2%	43.3%		80.9%	98.6%	
US_m2_s51_t10_c3	59 699	7	10		4	1		38.0%	37.0%		47.4%	46.0%		79.3%	84.6%	
US_m2_s51_t10_c4	59 879	7	9		4	2		38.0%	37.5%		47.5%	47.8%		79.4%	91.1%	
US_m2_s51_t15_c3	70 717	9	13		6	3		34.7%	35.0%		38.5%	47.3%		69.2%	83.9%	
US_m2_s51_t15_c4	70 082	12	12		6	3		40.3%	33.3%		42.1%	46.7%		74.6%	83.7%	
US_m2_s51_t20_c3	74 852	7	14		12	4		33.2%	29.5%		40.3%	43.4%		66.5%	76.2%	
US_m2_s51_t20_c4	76 892	7	14		12	5		32.5%	31.8%		45.3%	43.8%		69.6%	77.6%	
		Repr 1	Repr 2	Repr 3	Repr 1	Repr 2	Repr 3	Repr 1	Repr 2	Repr 3	Repr 1	Repr 2	Repr 3	Repr 1	Repr 2	Repr 3
US_m3_s51_t5_c3	52 596	6	4	5	0	2	0	41.0%	42.0%	34.0%	45.3%	44.7%	34.6%	88.8%	96.9%	97.2%
US_m3_s51_t5_c4	52 230	6	5	5	0	2	0	42.0%	47.0%	34.0%	49.7%	44.3%	41.8%	92.3%	99.4%	98.1%
US_m3_s51_t10_c3	68 004	10	6	6	1	5	5	36.0%	38.0%	36.5%	52.5%	42.5%	36.7%	77.3%	88.6%	98.8%
US_m3_s51_t10_c4	68 108	9	7	5	2	4	4	36.5%	38.0%	29.5%	47.0%	39.8%	43.0%	70.8%	87.8%	98.9%
US_m3_s51_t15_c3	80 373	10	10	8	5	6	6	33.7%	36.0%	30.0%	53.8%	42.6%	49.2%	73.1%	86.1%	93.6%
US_m3_s51_t15_c4	78 889	8	8	9	6	7	6	32.3%	33.7%	32.0%	46.5%	41.6%	48.0%	71.5%	81.8%	96.3%
US_m3_s51_t20_c3	85 305	9	7	7	8	10	6	28.2%	29.2%	21.5%	42.2%	36.5%	40.4%	64.7%	73.3%	80.3%
US_m3_s51_t20_c4	85 092	10	7	7	6	11	8	26.8%	30.8%	24.5%	49.3%	40.2%	43.0%	65.1%	75.7%	85.7%

$\Phi^{(\mathrm{inc})}$

Instance	Obj	# First activities			# Subsequent activities			Activity time (%)			Traveling time (%)			Budget consumption (%)		
		Repr 1			Repr 1			Repr 1			Repr 1			Repr 1		
US_m1_s51_t5_c3	28 547	7			0			48.0%			46.0%			88.6%		
US_m1_s51_t5_c4	28 547	7			0			48.0%			46.0%			88.6%		
US_m1_s51_t10_c3	40 355	11			0			38.5%			43.9%			77.4%		
US_m1_s51_t10_c4	40 355	11			0			38.5%			44.3%			77.5%		
US_m1_s51_t15_c3	48 931	16			0			36.3%			41.9%			70.4%		
US_m1_s51_t15_c4	47 887	15			0			34.3%			46.2%			72.2%		
US_m1_s51_t20_c3	56 723	22			0			36.5%			45.4%			70.5%		
US_m1_s51_t20_c4	57 600	23			0			38.0%			46.0%			70.6%		
		Repr 1	Repr 2		Repr 1	Repr 2		Repr 1	Repr 2		Repr 1	Repr 2		Repr 1	Repr 2	
US_m2_s51_t5_c3	45 559	8	5		0	0		56.0%	34.0%		34.7%	47.1%		89.9%	96.9%	
US_m2_s51_t5_c4	44 900	6	7		0	0		42.0%	48.0%		39.1%	46.3%		80.2%	98.6%	
US_m2_s51_t10_c3	59 531	11	13		0	0		37.0%	42.5%		51.5%	40.9%		77.0%	85.8%	
US_m2_s51_t10_c4	60 118	11	11		0	0		37.0%	36.0%		48.9%	44.9%		74.0%	82.2%	
US_m2_s51_t15_c3	61 312	13	14		1	2		31.0%	34.7%		46.1%	44.6%		64.6%	78.7%	
US_m2_s51_t15_c4	59 728	12	12		1	2		29.0%	30.7%		44.1%	51.4%		62.9%	79.7%	
US_m2_s51_t20_c3	62 774	14	15		2	3		26.2%	29.8%		42.4%	46.7%		57.6%	74.3%	
US_m2_s51_t20_c4	59 767	14	12		7	3		34.5%	24.5%		38.8%	44.6%		64.5%	65.5%	
		Repr 1	Repr 2	Repr 3	Repr 1	Repr 2	Repr 3	Repr 1	Repr 2	Repr 3	Repr 1	Repr 2	Repr 3	Repr 1	Repr 2	Repr 3
US_m3_s51_t5_c3	53 487	5	5	5	0	1	0	35.0%	42.0%	33.0%	54.5%	38.4%	36.8%	85.7%	96.3%	93.8%
US_m3_s51_t5_c4	52 492	7	6	5	0	1	0	48.0%	46.0%	33.0%	45.7%	44.1%	31.0%	85.3%	97.2%	97.7%
US_m3_s51_t10_c3	58 593	8	10	7	0	1	2	26.0%	36.5%	30.0%	51.9%	47.5%	35.6%	62.7%	83.4%	91.6%
US_m3_s51_t10_c4	63 120	9	10	7	1	1	1	33.5%	37.0%	25.5%	41.4%	44.0%	53.7%	68.6%	85.7%	98.5%
US_m3_s51_t15_c3	67 085	11	11	11	4	2	2	34.0%	27.7%	27.3%	44.1%	43.7%	43.5%	64.7%	72.4%	84.1%
US_m3_s51_t15_c4	63 767	11	10	10	4	3	4	33.0%	28.7%	30.7%	50.3%	52.2%	44.4%	67.5%	82.5%	97.4%
US_m3_s51_t20_c3	57 091	10	8	6	6	7	9	26.5%	25.2%	25.5%	42.4%	43.3%	31.7%	59.6%	70.5%	80.6%
US_m3_s51_t20_c4	60 760	11	8	8	5	8	8	26.2%	27.0%	26.8%	48.2%	42.6%	43.2%	59.8%	71.6%	88.6%

clustering states based on their resistance preserves inclusivity while increasing the overall complexity of the model. Furthermore, accounting for the heterogeneity of politicians leads to a more realistic model of election campaigns that better reflects the complexities of real-world political logistics.

Future research could expand on the RM-PRP in several directions. First, stochastic elements such as unpredictable rewards could be integrated into the model to better reflect real-world uncertainty. Another interesting direction could be developing dynamic optimization algorithms to adjust campaign itineraries based on live feedback and changing political landscapes, or exploring the competitive dynamics of simultaneous campaigns by multiple parties in overlapping states.

From a methodological perspective, our current matheuristic approach could be further enhanced by incorporating a metaheuristic

Table 9
Solution analysis for periodic reward profile ($\Phi^{(per)}$).

		$\Phi^{(per)}$														
Instance	Obj	# First activities			# Subsequent activities			Activity time (%)			Traveling time (%)			Budget consumption (%)		
		Repr 1			Repr 1			Repr 1			Repr 1			Repr 1		
US_m1_s51_t5_c3	22 630	6			0			42.0%			49.9%			95.4%		
US_m1_s51_t5_c4	22 630	6			0			42.0%			49.9%			95.4%		
US_m1_s51_t10_c3	37 548	9			2			38.5%			42.7%			75.3%		
US_m1_s51_t10_c4	37 548	9			2			38.5%			42.7%			75.3%		
US_m1_s51_t15_c3	49 301	12			3			34.7%			51.2%			75.5%		
US_m1_s51_t15_c4	50 234	11			4			35.0%			44.1%			75.4%		
US_m1_s51_t20_c3	60 267	15			6			36.2%			40.6%			72.0%		
US_m1_s51_t20_c4	59 639	15			5			34.2%			44.4%			73.6%		
		Repr 1	Repr 2		Repr 1	Repr 2		Repr 1	Repr 2		Repr 1	Repr 2		Repr 1	Repr 2	
US_m2_s51_t5_c3	36 193	6	6		0	1		42.0%	48.0%		50.0%	44.0%		95.0%	99.0%	
US_m2_s51_t5_c4	36 193	6	6		0	1		42.0%	48.0%		50.0%	44.0%		95.0%	99.0%	
US_m2_s51_t10_c3	56 820	10	6		1	5		37.0%	38.5%		43.4%	41.5%		75.4%	89.6%	
US_m2_s51_t10_c4	56 159	7	9		3	3		34.5%	41.0%		48.9%	44.6%		78.3%	91.2%	
US_m2_s51_t15_c3	63 031	8	12		7	3		34.3%	33.0%		41.1%	43.7%		75.9%	75.4%	
US_m2_s51_t15_c4	66 209	10	9		5	6		34.0%	34.0%		41.2%	37.9%		73.6%	78.9%	
US_m2_s51_t20_c3	72 683	12	13		7	6		32.0%	31.8%		46.4%	41.6%		64.4%	76.8%	
US_m2_s51_t20_c4	62 861	9	10		7	9		27.3%	32.2%		40.3%	44.5%		60.5%	79.2%	
		Repr 1	Repr 2	Repr 3	Repr 1	Repr 2	Repr 3	Repr 1	Repr 2	Repr 3	Repr 1	Repr 2	Repr 3	Repr 1	Repr 2	Repr 3
US_m3_s51_t5_c3	43 600	6	5	6	0	1	0	41.0%	42.0%	40.0%	45.5%	42.7%	32.9%	90.8%	98.6%	98.7%
US_m3_s51_t5_c4	42 777	6	5	6	0	1	0	42.0%	40.0%	40.0%	49.9%	55.8%	34.3%	95.4%	98.4%	98.1%
US_m3_s51_t10_c3	62 382	8	5	7	2	5	3	34.0%	34.5%	33.5%	47.3%	34.3%	39.0%	75.5%	75.2%	98.8%
US_m3_s51_t10_c4	60 199	8	7	7	2	4	3	33.5%	37.0%	33.5%	48.2%	44.2%	39.0%	74.2%	87.3%	98.8%
US_m3_s51_t15_c3	65 792	8	8	5	5	6	9	29.7%	31.3%	31.3%	49.0%	45.3%	40.4%	67.2%	82.7%	98.0%
US_m3_s51_t15_c4	64 932	8	9	7	6	5	6	30.7%	31.3%	29.7%	45.2%	45.3%	34.6%	65.4%	82.2%	90.6%
US_m3_s51_t20_c3	66 531	9	8	7	6	8	5	25.2%	27.8%	19.5%	40.3%	38.2%	35.3%	60.3%	70.5%	69.4%
US_m3_s51_t20_c4	68 576	9	9	7	6	10	4	25.2%	32.5%	17.8%	41.3%	35.9%	44.2%	61.9%	74.6%	73.3%

Table 10
Sensitivity analysis on budgets using the convex reward profile ($\Phi^{(cvx)}$).

		$\Phi^{(cvx)}$									
Instance	Obj	# First activities		# Subsequent activities		Activity time (%)		Traveling time (%)		Budget consumption (%)	
		Repr 1	Repr 2	Repr 1	Repr 2	Repr 1	Repr 2	Repr 1	Repr 2	Repr 1	Repr 2
US_m2_s51_t5_c3_budgets0.7	26 623	5	4	0	1	35.0%	34.0%	41.9%	29.9%	98.5%	99.9%
US_m2_s51_t5_c3_budgets0.8	30 295	5	4	1	1	42.0%	35.0%	36.4%	37.6%	98.8%	99.8%
US_m2_s51_t5_c3_budgets0.9	34 020	7	5	0	1	49.0%	41.0%	46.1%	40.7%	98.7%	99.4%
US_m2_s51_t5_c3_budgets1.0	35 010	6	6	1	1	49.0%	48.0%	42.8%	44.9%	89.3%	99.2%
US_m2_s51_t5_c3_budgets1.1	35 567	7	5	0	2	49.0%	49.0%	48.0%	43.0%	86.2%	94.7%
US_m2_s51_t5_c3_budgets1.2	35 567	7	5	0	2	49.0%	49.0%	48.0%	44.9%	79.0%	87.7%
US_m2_s51_t5_c3_budgets1.3	35 567	7	5	0	2	49.0%	49.0%	48.0%	43.0%	72.9%	80.2%

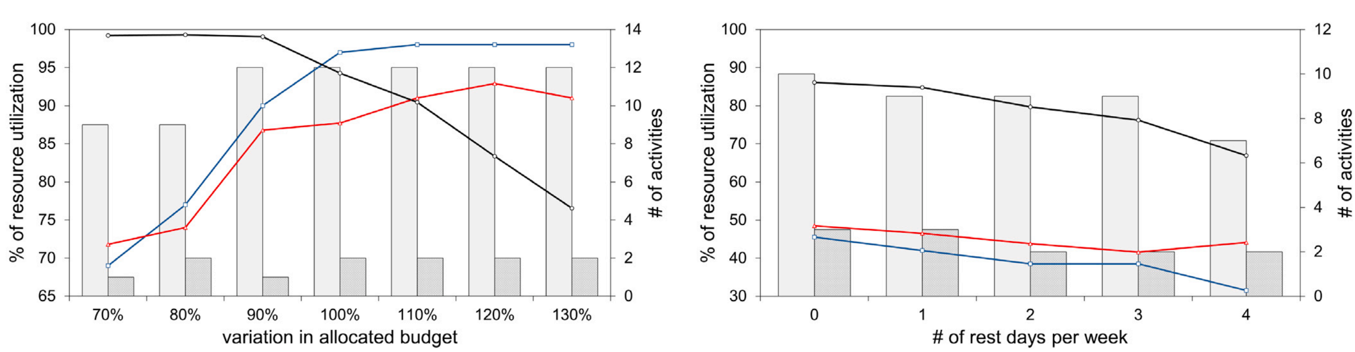

(a) (b)

Fig. 8. Sensitivity analysis on allocated budgets for instance *US_m2_s51_t5_c3* (left) and on weekly rest days for instance *US_m1_s51_t10_c4* (right) using the convex reward profile ($\Phi^{(cvx)}$).

layer or by embedding it in a general-purpose matheuristic framework that more directly uses the mathematical structure of the RM-PRP. In particular, methods such as kernel search or hybrid algorithms that integrate MIP-based components appear especially promising, given the complexity of the problem's constraints.

Table 11
Sensitivity analysis on rest days using the convex reward profile ($\Phi^{(\mathrm{cvx})}$).

	$\Phi^{(\mathrm{cvx})}$					
Instance	Obj	# First activities	# Subsequent activities	Activity time (%)	Traveling time (%)	Budget consumption (%)
		Repr 1	Repr 1	Repr 1	Repr 1	Repr 1
US_m1_s51_t10_c4_restdays0	39 134	10	3	45.5%	48.5%	86.1%
US_m1_s51_t10_c4_restdays1	38 600	9	3	42.0%	46.5%	84.8%
US_m1_s51_t10_c4_restdays2	36 640	9	2	38.5%	43.8%	79.7%
US_m1_s51_t10_c4_restdays3	34 346	9	2	38.5%	41.6%	76.2%
US_m1_s51_t10_c4_restdays4	29 983	7	2	31.5%	44.1%	66.9%

Another promising direction concerns the handling of subtour elimination constraints (SECs), which are introduced as lazy constraints in our model. As is common in routing problems, adding short-cycle SECs at the outset is often suggested to prevent early infeasibilities. However, in RM-PRP this led to a substantial increase in constraints and hindered performance in larger instances. Future work could explore hybrid selective insertion strategies based on reward thresholds or instance-specific features.

Finally, the RM-PRP framework could be adapted to other domains beyond political campaigning. Potential applications include humanitarian logistics, coordinated health interventions, large-scale marketing campaigns, and, in general, settings where limited resources must be allocated over time and space to maximize impact.

CRediT authorship contribution statement

Renata Mansini: Writing – review & editing, Writing – original draft, Visualization, Validation, Supervision, Project administration, Methodology, Investigation, Formal analysis, Conceptualization. **Lorenzo Moreschini:** Writing – review & editing, Writing – original draft, Visualization, Validation, Software, Methodology, Investigation, Formal analysis, Conceptualization. **Mesut Sayin:** Writing – review & editing, Writing – original draft, Visualization, Validation, Methodology, Investigation, Data curation, Conceptualization.

Declaration of competing interest

The authors declare that they have no known competing financial interests or personal relationships that could have appeared to influence the work reported in this paper.

Appendix. US instances generation

The RM-PRP incorporates parameters that can be adjusted to different electoral systems. Our test instances are based on the 2020 US presidential elections. In the following, we detail the methodology we applied to estimate the value of each parameter.

Cities (N) - We consider the 50 US state capitals plus the District of Columbia as the cities politicians can visit.

Base rewards ($\tilde{r}_{mi}$) - The base reward value $\tilde{r}_{mi} \in \mathbb{R}^+$ depends on the politician $m \in M$ and the city $i \in N$ and is computed as the product of four coefficients: the *Importance Index* (II_i), the *Resistance Index* (RI_i), the *Electoral Votes* (EV_i) and the *Politician Relevance* (PR_m). The US presidential election follows an indirect system known as the *Electoral College*, which consists of 538 total votes, with at least 270 required to win. A state's importance is primarily determined by its number of electoral votes [39] and its tendency to shift party preference (swing state). Other factors, such as voter demographics, media coverage, and fundraising probability, are more challenging to quantify and are partially encompassed within the coefficients we consider. Both the Democratic and Republican parties meticulously assess the criteria mentioned above as they make decisions on where to hold activities [40].

Table A.12
Positively and negatively critical states for Democrats and Republicans considering a variation of ±20% in the number of votes.

Democrats		Republicans	
−20%	+20%	−20%	+20%
Colorado	Alaska	Alaska	Colorado
Connecticut	Arizona	Arizona	Maine
Delaware	Florida	Florida	Michigan
Illinois	Indiana	Indiana	Minnesota
Maine	Iowa	Iowa	Nevada
Michigan	Georgia	Kansas	New Hampshire
Minnesota	Mississippi	Louisiana	New Jersey
Nevada	Missouri	Mississippi	New Mexico
New Hampshire	North Carolina	Missouri	Oregon
New Jersey	Ohio	Montana	Pennsylvania
New Mexico	South Carolina	Nebraska	Virginia
New York	Texas	North Carolina	Wisconsin
Oregon		Ohio	
Pennsylvania		South Carolina	
Virginia		Tennessee	
Washington		Texas	
Wisconsin			

The Importance Index (II_i) measures the significance of highly contested swing states, which can shift in favor of either party and strongly influence the election outcome. Key examples include Pennsylvania, Wisconsin, Michigan, and North Carolina, where both parties focus their campaign efforts. This index measures whether a vote shift alters a party's chances: a state is *positively important* if a vote increase secures a win, *negatively important* if it does not affect the party's chances of winning, and non-important otherwise. For instance, Kentucky holds little importance for Democrats, as even a 20% vote increase would not secure a win. On the other hand, North Carolina is highly significant, as a small vote gain could flip the state. We set II_i to 2, 2, and 1 for positively important, negatively important, and non-important states, respectively (see the criticality analysis performed in [9]). We analyzed vote sensitivity for Democrats and Republicans, assessing 1%–20% shifts and their impact on state outcomes to determine the importance index nationwide. Fig. A.9 illustrates the impact of vote variations on election outcomes from 2012 to 2020. States are highlighted when a vote shift alters the winning party. For example, a +1% Democratic vote change has minimal effect, while a +5% increase flips five Republican states. Table A.12 lists positively and negatively critical states for both parties at a 20% sensitivity threshold.

The Resistance Index (RI_i) quantifies a state's likelihood of changing its winning party, reflecting its historical voting stability. States with a long-standing allegiance to a party, such as Idaho (Republican since 1964), are highly resistant to change, making them difficult targets for the opposing party. Analyzing US presidential elections since 2000, we found that Florida and Iowa had the lowest resistance, switching parties three times. Michigan, Pennsylvania, Wisconsin, Ohio, Indiana, New Mexico, and North Carolina changed twice, while Arizona,

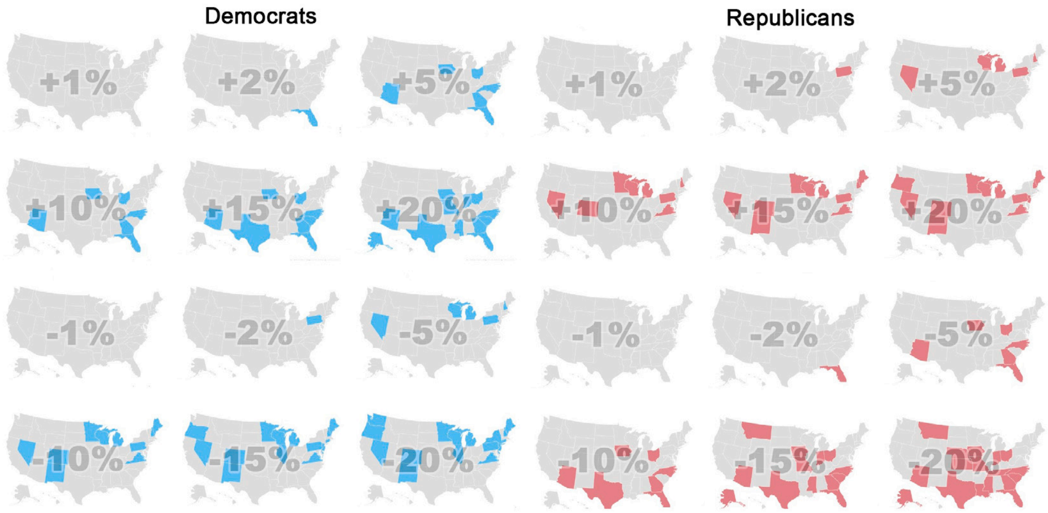

Fig. A.9. Sensitivity analysis of average popular votes based on the US presidential elections in 2012–2020.

Georgia, Colorado, Nevada, New Hampshire, and Virginia switched once. The remaining states showed the highest resistance, maintaining the same winning party for over two decades. These values have been computed normalizing the number of times a state has switched party on a scale ranging from 1 to 10.

The Electoral votes (EV_i) considers the number of electoral votes a state holds, which significantly influences campaign strategy. States with a higher number of electoral votes, such as New York, California, Illinois, Texas, Pennsylvania, and Arizona, are highly sought after, as winning them significantly increases the chances of securing the presidency and campaign resources are often prioritized for them. In our experiment, the value of EV_i is set to the number of electoral college votes assigned to the state of city $i \in N$.

The Politician Relevance (PR_i) reflects the varying impact of an activity depending on the politician performing it. For example, a speech by the presidential candidate has greater influence than one delivered by another party member. We set the index to 1, 0.9, and 0.75 for the first, second, and third politician, respectively.

Meeting durations (a_i) - Based on the 2020 US presidential elections, speech durations ranged from 30 min to 1 h, with no correlation to state population. We set meeting times between 180 and 210 min, including preparation time.

Travel times (d_{ij}) - We analyzed travel times between US state capitals using car, airplane, and a combination of both, considering the fastest mode of transport for each pair. The value of d_{ij} was set to the quickest transportation time, including 30 minutes for CIP check-ins and check-outs. This is the first analysis of its kind for the US.

Travel costs (c_{ij}) - The literature on routing and political science lacks specific data on election campaign travel expenses, with campaign finance reports from the Federal Election Commission providing only overall costs.[10] Due to the unavailability of detailed information, we turned to media sources and discovered that many presidential candidates use private companies like Air Partner for their travel.[11]

Throughout the years, a diverse range of aircraft has been employed in presidential campaigns. For instance, Mitt Romney utilized a former U2 360 tour plane, specifically an MD-83. Vice President Paul Ryan traveled in a 42-year-old DC-9. John McCain used a Boeing 737, whereas Obama, John Kerry in 2004, and George Bush in 2000 all relied on larger 757s. Sarah Palin's transportation in 2008 was an E190, while Ted Cruz and Marco Rubio, Republican rivals of Trump in 2016, both opted for Cessna Citations.[12] We focused on the operating costs of a Boeing 757, a commonly used aircraft in campaigns, with variable expenses estimated at 50 dollars per mile.[13] For car travel, we calculated average costs based on using 10 midibuses.

Meeting costs (h_i) - The cost of organizing a public speech during an election campaign includes venue rental, equipment, logistics, and security. Considering the Federal Election Commission information, we estimate a fixed cost of \$20,000, with an additional \$1,000 per electoral vote, increasing to \$2,000 for battleground states due to higher resource allocation.

Overnight stay costs (o_i) - These values are estimated based on the average price of 10 double rooms in a top-rated 5-star hotel, covering both the politician's entourage and security.

Politician budgets (b_m) - In US presidential elections, there are no restrictions on total spending. The 2020 US election spending was estimated at \$14.4 billion, with a significant portion spent on advertising and media. In our model, considering costs beyond those related to routing and scheduling, we estimate daily expenses of \$100,000 for the presidential candidate, \$80,000 for the second politician, and \$60,000 for the third.

Campaign planning horizon ($\bar{t}$) - The campaign rallies for Democrats and Republicans in the 2020 US presidential elections lasted 54 days and 77 days, respectively. Based on past campaign plans of both parties, we set the maximum value of $\bar{t}$ to 40 days.

Maximum number of meetings allowed in each period (p) - In the 2020 US presidential elections, the Republican candidate held a maximum of two daily speeches, with a total of three meetings if including debates. The Democratic candidate held up to four meetings daily, except for when they visited seven cities in Pennsylvania. Based on this, the parameter p was set to 2.

Minimum number of rest days (e, g) - Campaign schedules of politicians often incorporate rest days during which no official activity is conducted. In the 2020 elections, the Democratic and Republican candidates included 25 and 24 rest days, respectively, over the entire campaign period of 90 days. Consequently, we set the requirement of at least two rest days per week in each politician's schedule ($e = 2$, $g = 7$).

[10] https://www.fec.gov/data/elections

[11] https://www.airpartner.com/en/

[12] https://simpleflying.com/flying-the-candidates-inside-the-world-of-presidential-campaign-charters/

[13] https://www.avjetglobal.com/wp-content/uploads/2021/05/current_operating_costs_7_15_2019.pdf

Maximum number of consecutive days a politician is allowed to be absent from the campaign center (u) - Political experts suggest that, while frequent visits to the campaign center are not essential, candidates typically make regular visits for strategic purposes. Based on past itineraries, candidates return to the center every 7 to 15 days. In our experiments, we set this value to $u = 10$.

Number of clusters ($\bar{k}$) - We defined a maximum of $\bar{k} = 4$ clusters, namely N_1, N_2, N_3, and N_4, corresponding to states where the winning party has switched zero, one, two, and three times since the 2000 presidential elections, respectively. For instances with 3 clusters, N_2 and N_3 are merged into one.

Data availability

Data are publicly accessible at https://github.com/lmores/or-rmprp-data.

References

[1] Wlezien Christopher. Policy (mis) representation and the cost of ruling: US presidential elections in comparative perspective. Comp Political Stud 2017;50(6):711–38.
[2] Tricoire Fabien, Romauch Martin, Doerner Karl F, Hartl Richard F. Heuristics for the multi-period orienteering problem with multiple time windows. Comput Oper Res 2010;37(2):351–67.
[3] Vidigal Corrêa Victor Hugo, Dong Hang, Iori Manuel, dos Santos André Gustavo, Yagiura Mutsunori, Zucchi Giorgio. An iterated local search for a multi-period orienteering problem arising in a car patrolling application. Networks 2024;83(1):153–68.
[4] Engevall Stefan, Göthe-Lundgren Maud, Värbrand Peter. The heterogeneous vehicle-routing game. Transp Sci 2004;38(1):71–85.
[5] Zhang Qihuan, Wang Ziteng, Huang Min, Yu Yang, Fang Shu-Cherng. Heterogeneous multi-depot collaborative vehicle routing problem. Transp Res Part B: Methodol 2022;160:1–20.
[6] Devine Christopher J. What if hillary clinton had gone to wisconsin? Presidential campaign visits and vote choice in the 2016 election. Forum 2018;16(2):211–34.
[7] Pomper Gerald M. The presidential election. Taylor & Francis; 2013, p. 23.
[8] Nohlen Dieter, Stöver Philip. Elections in Europe. Nomos Verlagsgesellschaft mbH & Co. KG; 2010.
[9] Shahmanzari Masoud, Aksen Deniz, Salhi Saïd. Formulation and a two-phase matheuristic for the roaming salesman problem: Application to election logistics. European J Oper Res 2020;280(2):656–70.
[10] Shahmanzari Masoud, Mansini Renata. A learning-based granular variable neighborhood search for a multi-period election logistics problem with time-dependent profits. European J Oper Res 2024.
[11] Chao I-Ming, Golden Bruce L, Wasil Edward A. The team orienteering problem. European J Oper Res 1996;88(3):464–74.
[12] Souffriau Wouter, Vansteenwegen Pieter, Vanden Berghe Greet, Van Oudheusden Dirk. The multiconstraint team orienteering problem with multiple time windows. Transp Sci 2013;47(1):53–63.
[13] Panadero Javier, Juan Angel, Bayliss Christopher, Currie Christine. Maximizing reward from a team of surveillance drones: A simheuristic approach to the stochastic team orienteering problem. Eur J Ind Eng 2020;14(4):485–516.
[14] Juan AA, Freixes A, Panadero J, Serrat C, Estrada-Moreno A. Routing drones in smart cities: A biased-randomized algorithm for solving the team orienteering problem in real time. Transp Res Procedia 2020;47:243–50.
[15] Gavalas Damianos, Konstantopoulos Charalampos, Mastakas Konstantinos, Pantziou Grammati, Vathis Nikolaos. Heuristics for the time dependent team orienteering problem: Application to tourist route planning. Comput Oper Res 2015;62:36–50.
[16] Dang Duc-Cuong, Guibadj Rym Nesrine, Moukrim Aziz. An effective PSO-inspired algorithm for the team orienteering problem. European J Oper Res 2013;229(2):332–44.
[17] Shahmanzari Masoud, Aksen Deniz. A multi-start granular skewed variable neighborhood tabu search for the roaming salesman problem. Appl Soft Comput 2021;102:107024.
[18] Shahmanzari Masoud, Aksen Deniz, Salhi Saïd. Multi-period travelling politician problem: A hybrid metaheuristic solution method. J Oper Res Soc 2022;73(6):1325–46.
[19] Aksen Deniz, Shahmanzari Masoud. A periodic traveling politician problem with time-dependent rewards. In: Operations research proceedings 2016: selected papers of the annual international conference of the german operations research society (GOR), Helmut Schmidt University Hamburg, Germany, August 30-September 2, 2016. Springer; 2017, p. 277–83.
[20] Kinable Joris, Smeulders Bart, Delcour Eline, Spieksma Frits CR. Exact algorithms for the equitable traveling salesman problem. European J Oper Res 2017;261(2):475–85.
[21] Huang Yixiao, Zhao Lei, Van Woensel Tom, Gross Jean-Philippe. Time-dependent vehicle routing problem with path flexibility. Transp Res Part B: Methodol 2017;95:169–95.
[22] Pan Binbin, Zhang Zhenzhen, Lim Andrew. Multi-trip time-dependent vehicle routing problem with time windows. European J Oper Res 2021;291(1):218–31.
[23] Cao Chao, Xu Jinyun, Zhang Ji, Choset Howie, Ren Zhongqiang. Heuristic search for the orienteering problem with time-varying reward. In: Proceedings of the international symposium on combinatorial search, vol. 17, 2024, p. 11–9.
[24] Khodadadian Masoud, Divsalar Ali, Verbeeck Cedric, Gunawan Aldy, Vansteenwegen Pieter. Time dependent orienteering problem with time windows and service time dependent profits. Comput Oper Res 2022;143:105794.
[25] Allahyari Somayeh, Yaghoubi Saeed, Van Woensel Tom. The secure time-dependent vehicle routing problem with uncertain demands. Comput Oper Res 2021;131:105253.
[26] Gmira Maha, Gendreau Michel, Lodi Andrea, Potvin Jean-Yves. Managing in real-time a vehicle routing plan with time-dependent travel times on a road network. Transp Res Part C: Emerg Technol 2021;132:103379.
[27] Wang Yong, Wang Zheng, Hu Xiangpei, Xue Guiqin, Guan Xiangyang. Truck–drone hybrid routing problem with time-dependent road travel time. Transp Res Part C: Emerg Technol 2022;144:103901.
[28] Guo Xiaolong, Zhang Wei, Liu Bingbing. Low-carbon routing for cold-chain logistics considering the time-dependent effects of traffic congestion. Transp Res Part D: Transp Environ 2022;113:103502.
[29] Chakraborty Shuvabrata, Agarwal Yogesh K. Solving the team orienteering problem with nonidentical agents: A Lagrangian approach. Networks 2021;78(4):443–60.
[30] Ralphs Ted K, Kopman Leonid, Pulleyblank William R, Trotter Leslie E. On the capacitated vehicle routing problem. Math Program 2003;94:343–59.
[31] Miller CE, Tucker AW, Zemlin RA. Integer programming formulation of traveling salesman problems. J ACM 1960;7(4):326–9.
[32] Dantzig G, Fulkerson R, Johnson S. Solution of a large-scale traveling-salesman problem. J Oper Res Soc Am 1954;2(4):393–410.
[33] Pferschy Ulrich, Staněk Rostislav. Generating subtour elimination constraints for the TSP from pure integer solutions. Central Eur J Oper Res 2017;25:231–60.
[34] Boykov Y, Kolmogorov V. An experimental comparison of min-cut/max-flow algorithms for energy minimization in vision. IEEE Trans Pattern Anal Mach Intell 2004;26(9):1124–37.
[35] Klumpp Tilman, Polborn Mattias K. Primaries and the new hampshire effect. J Public Econ 2006;90(6–7):1073–114.
[36] Trent Judith S, Friedenberg Robert V. Political campaign communication: Principles and practices. Rowman & Littlefield; 2008.
[37] Huntington Samuel P. Democracy’s third wave. J Democr 1991;2(2):12–34.
[38] Morgenstern Scott. Patterns of legislative politics: Roll-call voting in Latin America and the United States. Cambridge University Press; 2003.
[39] Lichtman Allan J, Keilis-Borok Vladimir I. Pattern recognition applied to presidential elections in the united states, 1860-1980: Role of integral social, economic, and political traits. Proc Natl Acad Sci 1981;78(11):7230–4.
[40] Lichtman Allan J. The 2020 presidential election: How the keys are pointing. Soc Educ 2020;84(1):14–7.